Thin-Walled Structures 171 (2022) 108662

Contents lists available at ScienceDirect

Thin-Walled Structures

journal homepage: www.elsevier.com/locate/tws

Full length article

On the primary resonance of non-homogeneous orthotropic structures with viscous damping within shear deformation theory

A.H. Sofiyev [a,b,c,*], F. Turan [d], N. Kuruoğlu [e]

[a] Department of Civil Engineering of Engineering Faculty, Suleyman Demirel University, Isparta, Turkey
[b] Information Technology Research and Application Center Member of Consultancy Board of ITRAC Center, Istanbul Commerce University, Beyoglu 34445/Istanbul, Turkey
[c] Scientific Research Centers for Composition Materials of UNEC-Azerbaijan State Economic University, 1001/Baku, Azerbaijan
[d] Department of Civil Engineering of Faculty of Engineering, Ondokuz Mayıs University, Samsun, Turkey
[e] Department of Civil Engineering of Faculty of Engineering and Architecture, Istanbul Gelisim University, Istanbul, Turkey

ARTICLE INFO

Keywords:
Nonlinear forced vibration
Primary resonance
Non-homogeneity
Anisotropy
Multiple scales method
Excitation
Damping
SDT

ABSTRACT

This study is one of the first attempts on the nonlinear forced vibration behaviors of nonhomogeneous orthotropic (NHO) structural members with linear viscous damping at primary resonance within the shear deformation theory (SDT). First, mechanical properties of double curved systems consisting of NHO materials are mathematically modeled and nonlinear basic relations are established. Using these relations, nonlinear basic partial differential equations are derived and reduced to ordinary differential equations with second and third order nonlinearities by Galerkin procedure. Multiple-scales method is used to obtain the nonlinear forced vibration frequency–amplitude dependence of double curved NHO structural members with damping. After testing the correctness of the proposed methodology, the influences of non-homogeneity, damping, transverse shear deformations and anisotropy on nonlinear forced vibration frequencies for various structural members at the primary resonance are investigated and interpreted in detail.

1. Introduction

At the present stage of the development of science and technology, scientific and technological progress is impossible without the production of new non-standard materials with high technological and operational properties alongside traditional materials, and most importantly, without anticipating their application possibilities. Currently, the heterogeneous anisotropic materials play a leading role in the construction of new products that are used in many developed industries. In modern technology, plates, panels and shells made of homogeneous anisotropic materials as well as heterogeneous anisotropic materials are widely used as main structural elements, especially in aviation and spacecraft, rocket and shipbuilding, mechanical engineering and construction.

The fact that the new generation heterogeneous composite materials created by technological methods have predetermined properties increases the reliability of the structures, as well as decreasing the material consumption and the cost of the products. The inhomogeneity of elastic properties can occur both due to the technological processes in obtaining the structural elements and in the formation process of the body itself. Studying the mechanical behavior of inhomogeneous anisotropic structural elements reveals many important practical problems for researchers in which the true properties of materials are taken into account. Although it is quite complicated to mathematically model the heterogeneity and anisotropy of materials in various problems of solid mechanics, it also creates new physical, qualitative and quantitative effects. The direction of research on vibration and stability problems of inhomogeneous anisotropic structural elements is determined by the current demands of engineering practice, the need to develop solid mechanics theories, including mathematical models of constructions, and the development of analytical and numerical methods to solve specific problems. It should be especially noted some fundamental studies, which occupy an important place in the development of the mechanics of inhomogeneous bodies [1–4].

In the framework of the theories developed in the above-mentioned monographs, the properties of inhomogeneous anisotropic materials were modeled mathematically and the effects of inhomogeneity and anisotropy on the strength calculations of structural elements were presented in the studies of [5–9]. Advanced shell theories are used to obtain realistic results in the strength calculations of shell-type elements made of composite anisotropic materials. After the devoted efforts of scientists, various advanced shear deformation theories have been formed. The development of shear deformation theories has led to more realistic results on the nonlinear response of shallow shells composed of advanced materials [10–13].

Since structural elements consisting of homogeneous and inhomogeneous composites are applied in various advanced industries, including spacecraft, rockets, aviation technology and other areas of technology, they inevitably experience nonlinear oscillations. Among types of

* Correspondence to: Department of Civil Engineering of Engineering Faculty, Suleyman Demirel University, 32260 Isparta, Turkey.
E-mail address: abdullahavey@sdu.edu.tr (A.H. Sofiyev).

https://doi.org/10.1016/j.tws.2021.108662
Received 14 September 2021; Received in revised form 1 November 2021; Accepted 4 November 2021
Available online 8 December 2021

vibrations that can cause the most damage to structural elements is forced vibrations caused by periodic external excitation depending on the time. When shell-type structural members have significant dynamic displacements (due to non-linear deformations), this relationship can reveal a "resonant" phenomenon. This circumstance, which occurs in structural elements, has become the cause of many accidents, and sometimes serious disasters. Modeling and solving problems of forced vibration in a resonance not only solves the problems of forecasting, but also maximally prevents their detrimental effect on structural elements. A systematic presentation of various problems of nonlinear dynamics, including nonlinear forced vibrations of homogeneous plates, panels and shallow shells, was given in the monographs of Volmir [14] and Amabili [15]. These books present solutions to various problems of nonlinear vibrations (natural, forced, parametric) described by the Fopp–Karman equations for plates and the Marger equations for shallow shells. An invaluable resource for solving nonlinear problems of forced vibration, especially in resonance cases, is work of Nayfeh and Mook [16].

Due to the complication of the modeling of forced vibration problems for inhomogeneous structural elements, the number of works is very limited compared to other vibration types. In recent years, the number of studies on the solution of nonlinear forced vibration problems of functionally graded structural elements has been increasing. Du et al. [17] studied the nonlinear forced vibration of infinitely long functionally graded cylindrical shells using the Lagrangian theory and multiple scale method. In the studies of Sheng and Wang [18] and [19] were investigated primary resonance responses of functionally graded rotating cylindrical shells in thermal medium including nonlinear dynamics, quasi-periodic and chaotic responses based on Hamilton principle using von Kármán nonlinear theory and first-order shear deformation theory. Ave et al. [20] studied primary resonance of double-curved nanocomposite systems using improved nonlinear theory and multi-scales method. In the study of Amabili and Balasubramanian [21] were investigated the nonlinear forced vibrations of laminated composite conical shells using a high-order shear deformation theory that include rotary inertia and geometric nonlinearity at all kinematic parameters and trigonometric extensions. Sofiyev et al. [22,23] presented the nonlinear forced vibration behaviors of functionally graded and nano-composites structural systems based on the classical shell theory (CST). In the study of Zhu et al. [24], the nonlinear free and forced vibrations of porous piezoelectric doubly curved shells resting on visco-elastic foundation is performed within nonuniform electric field model, harmonic balance and Runge–Kutta methods. Ye and Wang [25] analyzed the nonlinear forced vibration of thin-walled metal foam cylindrical shells reinforced with functionally graded graphene platelets, noting 1:1:1:2 internal resonances using the pseudo-arclength continuation technique. In a study by Liu et al. [26] used Donnell's nonlinear theory of shallow shells, Hamilton's principle, energy approximation, Galerkin scheme, and arc length continuation method for nonlinear forced vibrations of multilayer cylindrical shells made of porous functionally graded material (FGM) on an elastic substrate. In the study of Gao et al. [27], the symplectic wave-based method has been extended to free and forced vibration analysis of thin orthotropic circular cylindrical shells with arbitrary boundary conditions. Ahmadi et al. [28] investigated the non-linear forced vibrations of stiffened imperfect functionally graded double curved shallow shells, as rested on nonlinear elastic foundations using the CST.

The majority of aforementioned studies are devoted to the forced vibration of structural elements made of nonhomogeneous isotropic materials. Solutions of the forced vibration problems of the structural elements made of NHO materials are presented only within CST. The main purpose of this study is to solve this problem using the Galerkin procedure and the multiple scales method after mathematically modeling of this problem in the framework of SDT, considering the viscous damping effect, in order to obtain a damped nonlinear forced vibration frequency–amplitude dependence and an expression for the ratio of vibrations. This research is one of the first attempts to investigate the nonlinear forced vibration for NHO structural elements with viscous damping in the framework of SDT at primary resonance. Since the special cases of shells with double curvature are structural elements, such as spherical and hypar shells, rectangular plates and panels, obtained expressions can be used for their forced vibration analysis. In addition, it aims to analyze and interpret the quantitative and qualitative changes caused by the influences of non-homogeneity, nonlinearity, orthotropy, external excitation and viscous damping on the frequency–amplitude dependence.

2. Formulation of the problem

Let us consider the nonhomogeneous orthotropic double curved shallow shell with thickness h, side lengths l_1 and l_2, curvature radii R_1 and R_2, subjected to the harmonic external excitation $q(x, y, \tau)$ (see, Fig. 1). The orthogonal coordinate system is placed on the mid-surface of the double curved shell, its origin being situated at the upper left corner and the direction of the axes is shown in Fig. 1. We will denote the displacements in the direction of the x, y and z coordinate axes with symbols u, v and w, respectively. The shallow shell with double curvature is transformed into (a) spherical shell as $R_1 = R_2$, (b) hyperbolic-paraboloid shell or hypar shell as $R_1 = -R_2$, and (c) panel as $R_1 \to \infty$, and (d) plate, as $R_1 \to \infty,\ R_2 \to \infty$ (Fig. 2).

The elastic properties of shell-type structural elements made of NHO materials can be modeled as a continuous function of the z coordinate in the following form [5–9]:

$$E_{ii}^{\overline{z}} = \eta_1(\overline{z})E_{\mathrm{ii}}^0,\ \ G_{ij}^{\overline{z}} = \eta_1(\overline{z})G_{ij}^0,\ \ \rho_{HT}^{\overline{z}} = \eta_2(\overline{z})\rho^0, (i = 1,2, j = 2,3)\overline{z} = z/h \tag{1}$$

where $E_{ii}^0 (i = 1,2)$ are the elasticity moduli of raw materials in x and y directions, respectively, $G_{ij}^0 (i = 1,2, j = 2,3)$ are the shear moduli and ρ^0 is the density of raw materials.

2.1. Governing relations

The relationship between stress $(\sigma_1, \sigma_2, \sigma_{12}, \sigma_{13}, \sigma_{23})$ and strain $(\varepsilon_1, \varepsilon_2, \gamma_{12}, \gamma_{13}, \gamma_{23})$ tensors of shell-type structural elements made of NHO materials in the framework of SDT are formed as follows [14]:

$$\begin{pmatrix}\sigma_1\\ \sigma_2\\ \sigma_{12}\\ \sigma_{13}\\ \sigma_{23}\end{pmatrix} = \begin{bmatrix} Y_{11}^{\overline{z}} & Y_{12}^{\overline{z}} & 0 & 0 & 0\\ Y_{21}^{\overline{z}} & Y_{22}^{\overline{z}} & 0 & 0 & 0\\ 0 & 0 & Y_{66}^{\overline{z}} & 0 & 0\\ 0 & 0 & 0 & Y_{55}^{\overline{z}} & 0\\ 0 & 0 & 0 & 0 & Y_{44}^{\overline{z}}\end{bmatrix}\begin{bmatrix}\varepsilon_1\\ \varepsilon_2\\ \gamma_{12}\\ \gamma_{13}\\ \gamma_{23}\end{bmatrix} \tag{2}$$

where

$$Y_{ii}^{\overline{z}} = \frac{E_{ii}^{\overline{z}}}{1-\nu_{12}\nu_{21}} (\mathrm{i} = 1,2),\ \ Y_{12}^{\overline{z}} = \frac{\nu_{21}E_{11}^{\overline{z}}}{1-\nu_{12}\nu_{21}} = \frac{\nu_{12}E_{22}^{\overline{z}}}{1-\nu_{12}\nu_{21}} = Y_{21}^{\overline{z}},$$
$$Y_{44}^{\overline{z}} = G_{23}^{\overline{z}},\ \ Y_{55}^{\overline{z}} = G_{13}^{\overline{z}},\ \ Y_{66}^{\overline{z}} = G_{12}^{\overline{z}} \tag{3}$$

in which $\nu_{ij} (i, j = 1,2)$ denote the Poisson ratios for NHO materials and they are assumed to be constant and satisfies the condition $\nu_{21}E_{11}^{\overline{z}} = \nu_{12}E_{22}^{\overline{z}}$.

On the basis of the assumptions of the SDT, the $\sigma_{i3} (i = 1,2)$ can be expressed by the rotation angles of the normal to the reference surface $\chi_i (i = 1,2)$ and the shear stress functions $\overline{f}_i^z$ as follows [10]:

$$\sigma_{i3} = \overline{f}_i^z \chi_i, (i = 1,2) \tag{4}$$

where $\overline{f}_i^z = \frac{\mathrm{d}f_i^z}{\mathrm{d}z} (i = 1,2)$.

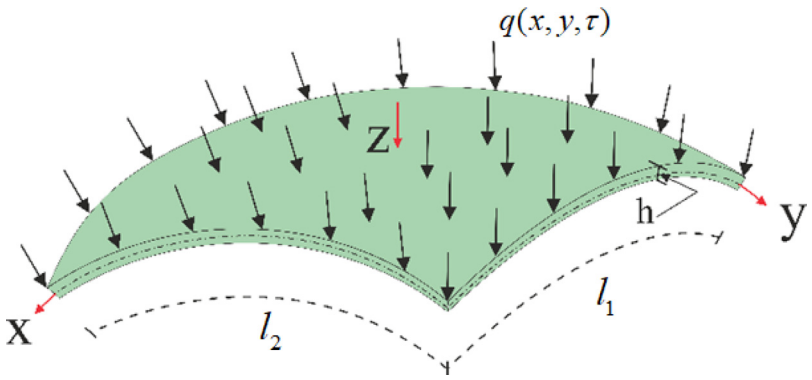

Fig. 1. NHO double curved shell subjected to external excitation and coordinate systems.

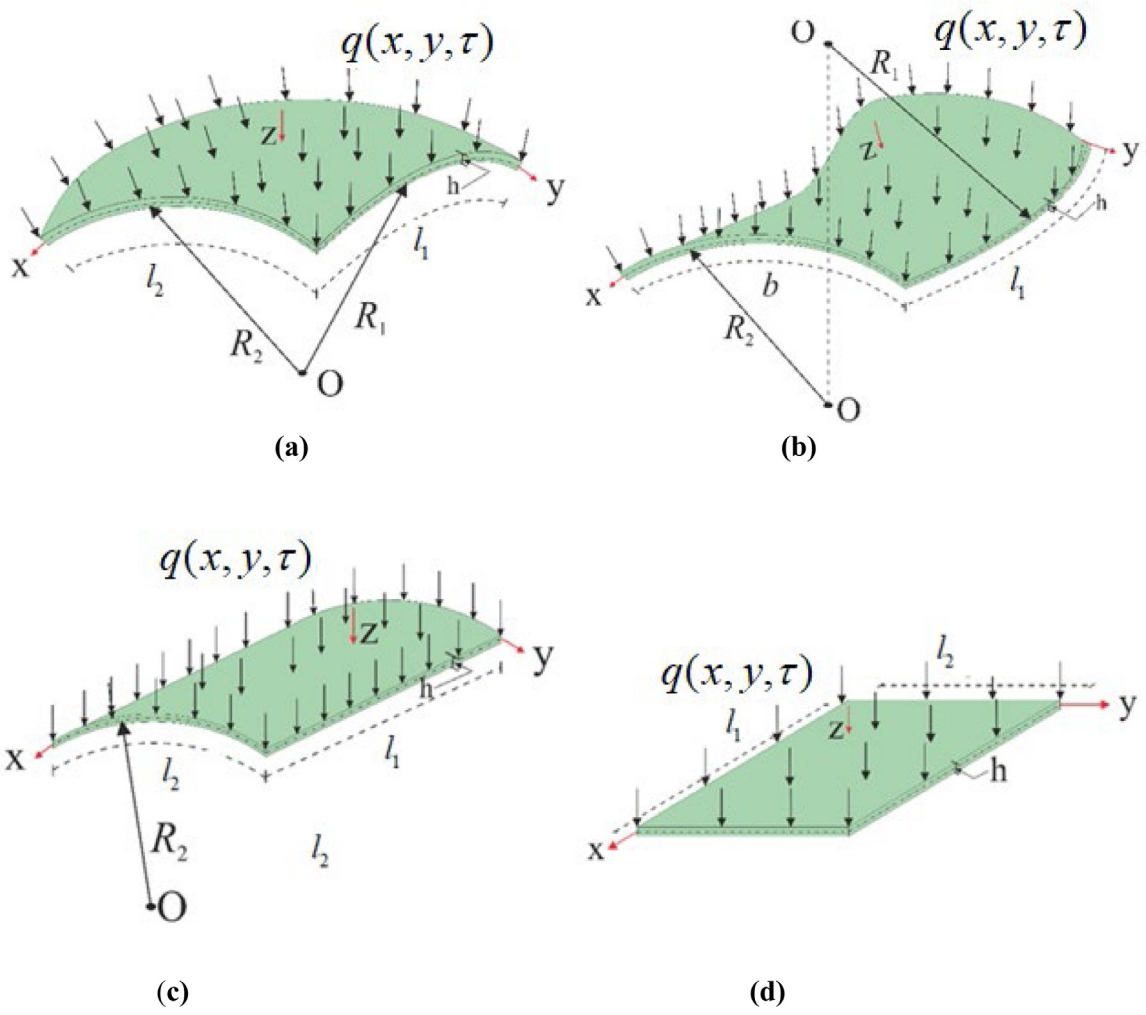

Fig. 2. (a) Spherical, (b) hyperbolic-paraboloid shells, (c) panel, (d) plate under an external excitation $q(\tau)$ and coordinate system.

The mathematical model of the stress functions corresponding to the distribution of transverse shear stresses in the thickness direction is as follows [10,11]:

$$\overline{f}_i^z = \frac{\mathrm{d}f_i^z}{\mathrm{d}z} = 1 - \overline{z}^2 \tag{5}$$

Two- and three-dimensional distributions of shear stress functions of structural elements are presented in Fig. 3.

The strains $(\varepsilon_1, \varepsilon_2, \gamma_{12})$ for any point of shells made from NHO materials can be expressed by stresses $(e_1, e_2, \gamma_{12}^0)$ at the reference surface, curvatures and rotation angles $\chi_i, (i = 1, 2)$, in the context of nonlinear Donnell-type shell theory and taking into account expression (4), as follows [14,15]:

$$\begin{bmatrix} \varepsilon_1 \\ \varepsilon_2 \\ \gamma_{12} \end{bmatrix} = \begin{bmatrix} e_1 - z\dfrac{\partial^2 w}{\partial x^2} + I_1^z \dfrac{\partial \chi_1}{\partial x} \\ e_2 - z\dfrac{\partial^2 w}{\partial y^2} + I_2^z \dfrac{\partial \chi_2}{\partial y} \\ \gamma_{12}^0 - 2z\dfrac{\partial^2 w}{\partial x \partial y} + I_1^z \dfrac{\partial \chi_1}{\partial y} + I_2^z \dfrac{\partial \chi_2}{\partial x} \end{bmatrix} \tag{6}$$

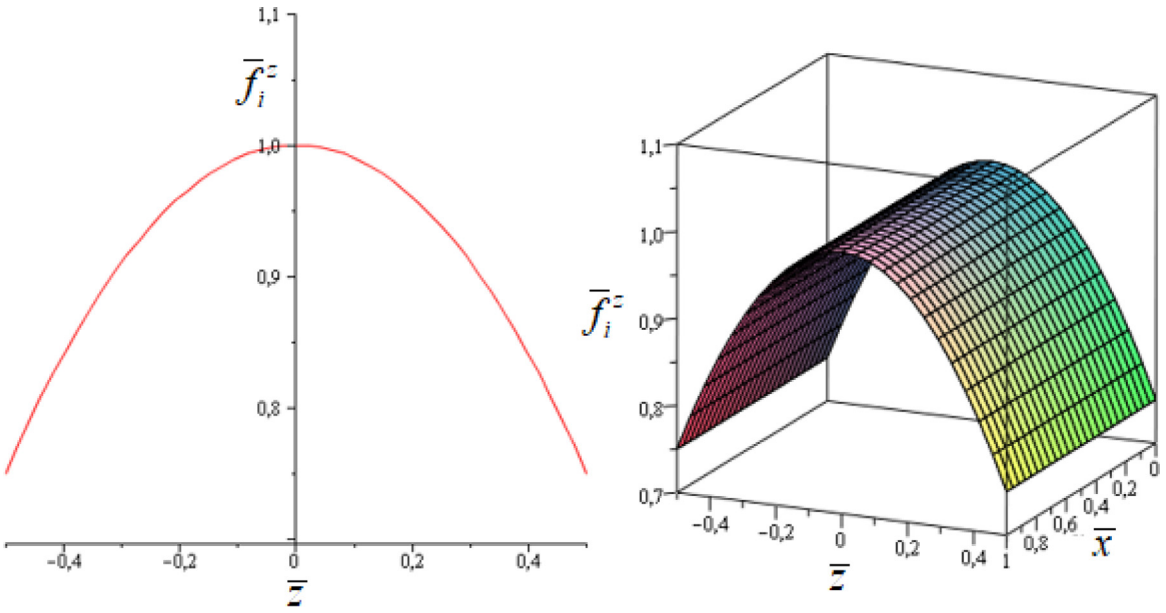

Fig. 3. (a) Two- and (b) three-dimensional distributions of transverse shear stress functions.

in which

$$\begin{bmatrix} e_1 \\ e_2 \\ \gamma_{12}^0 \end{bmatrix} = \begin{bmatrix} \frac{\partial u}{\partial x} - \frac{w}{R_1} + \frac{1}{2}\left(\frac{\partial w}{\partial x}\right)^2 \\ \frac{\partial v}{\partial y} - \frac{w}{R_2} + \frac{1}{2}\left(\frac{\partial w}{\partial y}\right)^2 \\ \frac{\partial v}{\partial x} + \frac{\partial u}{\partial y} + \frac{\partial w}{\partial x}\frac{\partial w}{\partial y} \end{bmatrix} \tag{7a}$$

$$I_1^z = \int_0^z \frac{1}{G_{23}^{\bar{z}}} \frac{\mathrm{d}f_1^z}{\mathrm{d}z}\mathrm{d}z, \quad I_2^z = \int_0^z \frac{1}{G_{13}^{\bar{z}}} \frac{\mathrm{d}f_2^z}{\mathrm{d}z}\mathrm{d}z \tag{7b}$$

If (6) is introduced in (2), it will be:

$$\begin{bmatrix} \sigma_1 \\ \sigma_2 \\ \gamma_{12} \end{bmatrix} = \begin{bmatrix} Y_{11}^{\bar{z}} & Y_{12}^{\bar{z}} & 0 \\ Y_{21}^{\bar{z}} & Y_{22}^{\bar{z}} & 0 \\ 0 & 0 & Y_{66}^{\bar{z}} \end{bmatrix} \begin{bmatrix} e_1 - z\frac{\partial^2 w}{\partial x^2} + I_1^z \frac{\partial \chi_1}{\partial x} \\ e_2 - z\frac{\partial^2 w}{\partial y^2} + I_2^z \frac{\partial \chi_2}{\partial y} \\ \gamma_{12}^0 - 2z\frac{\partial^2 w}{\partial x \partial y} + I_1^z \frac{\partial \chi_1}{\partial y} + I_2^z \frac{\partial \chi_2}{\partial x} \end{bmatrix} \tag{8}$$

The forces $(T_1, T_2, T_{12}), (Q_1, Q_2)$ and moments (M_1, M_2, M_{12}) of NHO structural elements are defined by the following integrals [15,16]:

$$\begin{aligned} (T_i, M_i) &= \int_{-h/2}^{h/2} (1, z)\,\sigma_i \mathrm{d}z, \ (Q_1, Q_2) = \int_{-h/2}^{h/2} (\sigma_{1k}, \sigma_{2k})\,\mathrm{d}z, \\ (T_{12}, M_{12}) &= \int_{-h/2}^{h/2} (1, z)\,\sigma_{12}\mathrm{d}z, (i = 1, 2, k = 2, 3) \end{aligned} \tag{9}$$

By introducing the Airy stress function, φ, the forces can be expressed as [15]:

$$(T_1, T_2, T_{12}) = h\left(\frac{\partial^2 \varphi}{\partial y^2}, \frac{\partial^2 \varphi}{\partial x^2}, -\frac{\partial^2 \varphi}{\partial x \partial y}\right) \tag{10}$$

The dynamic stability and deformation compatibility equations of double curved structures subjected to external excitation $q(x, y, \tau)$ and considering viscous damping effect based on the Hamilton principle are as follows [15]:

$$\frac{\partial M_1}{\partial x} + \frac{\partial M_{12}}{\partial y} - Q_1 + \rho_1 \frac{\partial^3 w}{\partial x \partial \tau^2} - \rho_2 \frac{\partial^2 \chi_1}{\partial \tau^2} = 0$$

$$\frac{\partial M_{21}}{\partial x} + \frac{\partial M_2}{\partial y} - Q_2 + \rho_1 \frac{\partial^3 w}{\partial y \partial \tau^2} - \rho_3 \frac{\partial^2 \chi_2}{\partial \tau^2} = 0 \tag{11}$$

$$\frac{\partial Q_1}{\partial x} + \frac{\partial Q_2}{\partial y} + \frac{T_1}{R_1} + \frac{T_2}{R_2} + T_1 \frac{\partial^2 w}{\partial x^2} + 2T_{12}\frac{\partial^2 w}{\partial x \partial y} + T_2 \frac{\partial^2 w}{\partial y^2} + q(x, y, \tau) = \rho_t \frac{\partial^2 w}{\partial \tau^2} + 2\xi \rho_t \frac{\partial w}{\partial \tau}$$

$$\frac{\partial^2 e_1}{\partial y^2} + \frac{\partial^2 e_2}{\partial x^2} - \frac{\partial^2 \gamma_{12}^0}{\partial x \partial y} = \left(\frac{\partial^2 w}{\partial x \partial y}\right)^2 - \frac{\partial^2 w}{\partial x^2}\frac{\partial^2 w}{\partial y^2} - \left(\frac{1}{R_2}\frac{\partial^2 w}{\partial x^2} + \frac{1}{R_1}\frac{\partial^2 w}{\partial y^2}\right) \tag{12}$$

where ρ_t and $\rho_i (i = 1, 2, 3)$ denote coefficients of normal and rotary inertia and are expressed as:

$$\begin{aligned} \rho_t &= \rho^0 \int_{-h/2}^{h/2} \eta_2(\bar{z})\mathrm{d}z, \ \rho_1 = \rho^0 \int_{-h/2}^{h/2} z^2 \eta_2(\bar{z})\mathrm{d}z, \\ \rho_2 &= \rho^0 \int_{-h/2}^{h/2} z I_1^z \eta_2(\bar{z})\mathrm{d}z, \ \rho_3 = \rho^0 \int_{-h/2}^{h/2} z I_2^z \eta_2(\bar{z})\mathrm{d}z \end{aligned} \tag{13}$$

We now substitute (8) and (10) into Eq. (9) and perform the integration over the thickness of the shell with a double curvature. The results of these mathematical operations are obtained the expressions for the strains on the mid-surface, forces and moments as the functions of the $\varphi, w, \chi_1, \chi_2$. The expressions for moments, forces and strains on the mid-surface are substituted into Eqs. (11) and (12) by considering the relation (10), the following set of equations for the dynamic stability and deformation compatibility equations for double curved shells made of NHO materials with viscous damping under external excitation $q(x, y, \tau)$ are obtained:

$$\begin{aligned} &L_{11}(\varphi) + L_{12}(w) + L_{13}(\chi_1) + L_{14}(\chi_2) = 0 \\ &L_{21}(\varphi) + L_{22}(w) + L_{23}(\chi_1) + L_{24}(\chi_2) = 0 \\ &L_{31}(\varphi) + L_{32}(w) + L_{33}(\chi_1) + L_{34}(\chi_2) + L_{35}(\varphi, w) + q(x, y, \tau) = \rho_t \frac{\partial^2 w}{\partial \tau^2} + 2\xi \rho_t \frac{\partial^2 w}{\partial \tau} \end{aligned} \tag{14}$$

$$L_{41}(\varphi) + L_{42}(w) + L_{43}(\chi_1) + L_{44}(\chi_2) + L_{45}(w, w) = 0 \tag{15}$$

where $L_{ij} (i = 1, 2, \ldots, 4, j = 1, 2, \ldots, 5)$ denote nonlinear differential operators and are given in Appendix A.

3. Methods of solution

The NHO shell-type structural elements with a double curvature under simply supported boundary conditions:

$$\begin{aligned} &w=0,\ \ M_1=0,\ \ \chi_2=0,\ \ \text{as } x=0 \text{ and } x=l_1\\ &w=0,\ \ M_2=0,\ \ \chi_1=0,\ \ \text{as } y=0 \text{ and } y=l_2 \end{aligned} \tag{16}$$

Thus, the functions w, χ_1 and χ_2 are sought in the following form [10,23]:

$$\begin{aligned} &w=\overline{w}(\tau)\sin(\overline{m}x)\sin(\overline{n}y),\ \ \chi_1=\overline{\chi}_1(\tau)\cos(\overline{m}x)\sin(\overline{n}y),\\ &\chi_2=\overline{\chi}_2(\tau)\sin(\overline{m}x)\cos(\overline{n}y) \end{aligned} \tag{17}$$

where $\overline{w}(\tau)$, $\overline{\chi}_i(\tau)(i=1,2)$ are the time dependent functions, $\overline{m}=\frac{m\pi}{l_1}$ and $\overline{n}=\frac{n\pi}{l_2}$, in which (m,n) is a vibration mode.

The expressions (17) are substituted in the partial differential Eq. (15) and the following expression for the φ is obtained depending on the deflection and rotation angles functions:

$$\varphi=\Lambda_1\cos(2\overline{m}x)+\Lambda_2\cos(2\overline{n}y)+\Lambda_3\sin(\overline{m}x)\sin(\overline{n}y) \tag{18}$$

where

$$\begin{aligned} &\Lambda_1=\frac{\overline{w}^2}{32B_{22}h}\left(\frac{\overline{n}}{\overline{m}}\right)^2,\ \ \Lambda_2=\frac{\overline{w}^2}{32B_{11}h}\left(\frac{\overline{n}}{\overline{m}}\right)^{-2},\\ &\Lambda_3=\frac{\delta_1\overline{w}^2+\delta_2\overline{\chi}_1+\delta_3\overline{\chi}_2}{h\left[B_{11}\overline{m}^4+(B_{12}+B_{21}+B_{31})\overline{m}^2\overline{n}^2+B_{22}\overline{n}^4\right]} \end{aligned} \tag{19}$$

in which

$$\begin{aligned} &\delta_1=B_{23}\overline{m}^4+(B_{24}+B_{13}-B_{32})\overline{m}^2\overline{n}^2+B_{14}\overline{n}^4+\frac{\overline{m}^2}{R_2}+\frac{\overline{n}^2}{R_1},\\ &\delta_2=-B_{25}\overline{m}^3-(B_{15}+B_{35})\overline{m}\overline{n}^2,\ \ \delta_3=-(B_{28}+B_{38})\overline{m}^2\overline{n}-B_{18}\overline{n}^3. \end{aligned} \tag{20}$$

Suppose that the excitation is unevenly distributed over the surface of the shell as follows:

$$q(x,y,\tau)=q_0\sin(\overline{m}x)\sin(\overline{n}y)\cos(\Omega\tau) \tag{21}$$

where Ω is the frequency and q_0 is the amplitude of excitation.

Taking into account (17), (18) and (21) and using the Galerkin method to the system of Eqs. (14), one gets,

$$\begin{aligned} &k_{11}^{\tau}\frac{\mathrm{d}^2\overline{w}}{\mathrm{d}\tau^2}+k_{12}^{\tau}\frac{\mathrm{d}^2\overline{\chi}_1}{\mathrm{d}\tau^2}+k_{11}\overline{w}+k_{11}^{NL}\overline{w}^2+k_{12}\overline{\chi}_1+k_{13}\overline{\chi}_2=0,\\ &k_{21}^{\tau}\frac{\mathrm{d}^2\overline{w}}{\mathrm{d}\tau^2}+k_{23}^{\tau}\frac{\mathrm{d}^2\overline{\chi}_2}{\mathrm{d}\tau^2}+k_{21}\overline{w}+k_{21}^{NL}\overline{w}^2+k_{22}\overline{\chi}_1+k_{23}\overline{\chi}_2=0,\\ &\rho_t\frac{\mathrm{d}^2\overline{w}}{\mathrm{d}\tau^2}+2\xi\rho_t\frac{\partial^2 w}{\partial\tau}+k_{31}\overline{w}+k_{31}^{NL}\overline{w}^2+k_{32}\overline{w}^3+k_{33}\overline{\chi}_1+k_{34}\overline{\chi}_2\\ &\quad-q_0\cos(\Omega\tau)=0 \end{aligned} \tag{22}$$

where $k_{ij}(i=1,2,3,j=1,2,3,4)$ are defined in Appendix B.

Analyzes show that inertia terms with the upper index τ have very little effect on the nonlinear vibration frequency values, so these terms (22) are ignored from the set of equations. Then, $\overline{\chi}_1$ and $\overline{\chi}_2$ functions in the first and second equations of the system are expressed with the $\overline{w}$ function and taken into account in the third equation of the Eq. (22), the following nonlinear ordinary differential equation is obtained:

$$\frac{\mathrm{d}^2\overline{w}}{\mathrm{d}\tau^2}+2\xi\frac{\mathrm{d}\overline{w}}{\mathrm{d}\tau}+\left(\omega_{SDT}^{Lin}\right)^2\overline{w}+\theta_1\overline{w}^2+\theta_2\overline{w}^3-\theta_3q_0\cos(\Omega\tau)=0 \tag{23}$$

where ω_{SDT}^{Lin} denotes the undamped linear frequency for NHO double curved structures in the framework of SDT and is defined by:

$$\omega_{SDT}^{Lin}=\sqrt{\frac{1}{\rho_t}\left[k_{31}-\frac{k_{21}k_{34}}{k_{23}}+\left(k_{33}-\frac{k_{22}k_{34}}{k_{23}}\right)\frac{k_{11}k_{23}-k_{21}k_{13}}{k_{22}k_{13}-k_{23}k_{12}}\right]} \tag{24}$$

and

$$\begin{aligned} &\theta_1=\frac{k_{31}^{*NL}}{\rho_t},\ \ \theta_2=\frac{k_{32}}{\rho_t},\ \ \theta_3=\frac{1}{\rho_t},\\ &k_{31}^{*NL}=k_{31}^{NL}-\frac{k_{34}k_{21}^{NL}}{k_{23}}+\left(\frac{k_{34}k_{22}}{k_{23}}-k_{33}\right)\frac{k_{11}^{NL}k_{23}-k_{13}k_{21}^{NL}}{k_{12}k_{23}-k_{13}k_{22}} \end{aligned} \tag{25}$$

The following initial conditions are used to solve the Eq. (23) [15,16,19,23,29]:

$$\overline{w}=\overline{w}_0\quad\text{and}\quad\frac{\mathrm{d}\overline{w}}{\mathrm{d}\tau}=0\quad\text{when}\quad\tau=0 \tag{26}$$

where $\overline{w}_0$ is the initial deflection amplitude.

Nonlinearity causes the formation of a term containing $\cos(\omega_{SDT}^{Lin}\tau)$ for $O(\varepsilon^3)$, which describes the small disturbance parameter. So, to ensure that all terms of (23) are of the same order, we express $2\xi\frac{\mathrm{d}\overline{w}}{\mathrm{d}\tau}$, as the $2\overline{\xi}_1\frac{\mathrm{d}\overline{w}}{\mathrm{d}\tau}$, and $\theta_3q_0\cos(\Omega\tau)$, as the $\varepsilon^2\overline{q}_0\cos(\Omega\tau)$, which can be transformed to the following form:

$$\frac{\mathrm{d}^2\overline{w}}{\mathrm{d}\tau^2}+\left(\omega_{SDT}^{Lin}\right)^2\overline{w}=-2\varepsilon^2\overline{\xi}_1\frac{\mathrm{d}\overline{w}}{\mathrm{d}\tau}-\varepsilon\overline{\theta}_1\overline{w}^2-\varepsilon^2\overline{\theta}_2\overline{w}^3+\varepsilon^2\overline{q}_0\cos(\Omega\tau) \tag{27}$$

where

$$\overline{\xi}_1=\frac{\xi}{\varepsilon^2},\ \ \overline{\theta}_1=\frac{\theta_1}{\varepsilon},\ \ \overline{\theta}_2=\frac{\theta_2}{\varepsilon^2},\ \ \overline{q}_0=\frac{\theta_3q_0}{\varepsilon^2} \tag{28}$$

For the solution of Eq. (27), the $\overline{w}$ is expanded into the series with a small parameter using the new time scales as follows [16,29]:

$$\overline{w}(\tau,\varepsilon)=\sum_{i=0}^{\infty}\varepsilon^i\overline{w}_i(\tau_0,\tau_1,\tau_2) \tag{29}$$

Here, $\tau_i=\varepsilon^i\tau(i=0,1,2,\ldots)$ denote new independent variables, which $\tau_0=\tau$ is a fast time characterizing the movements of linear vibrations with natural frequency, $\tau_1=\varepsilon\tau$ and $\tau_2=\varepsilon^2\tau$ are slow scales characterizing the amplitude and phase modulation in nonlinear vibration.

The integer expansions of derivatives, which are used in the method of multiple time scales, generally are written as [19,29]:

$$\begin{aligned} &\frac{\mathrm{d}}{\mathrm{d}t}=\sum_{i=0}^{\infty}D_i\varepsilon^i\\ &\frac{\mathrm{d}^2}{\mathrm{d}t^2}=D_0^2+2\varepsilon D_0D_1+\varepsilon^2(D_1^2+2D_0D_2)+\cdots \end{aligned} \tag{30}$$

where

$$D_0=\frac{\partial}{\partial\tau_0},\ \ D_1=\frac{\partial}{\partial\tau_1}\ \text{and}\ D_2=\frac{\partial}{\partial\tau_2} \tag{31}$$

For consistency the $\Omega-\omega_{SDT}^{Lin}$ is assumed to be $O(\varepsilon^2)$ and defined by:

$$\Omega=\omega_{SDT}^{Lin}+\varepsilon^2\vartheta \tag{32}$$

where ϑ is a detuning parameter that characterizes a small inconsistency between the frequency values.

After substituting expressions (29) and (30) into Eq. (27), coefficients with same powers of ε are set equal to zero, and the following equations are obtained for different orders:

$$\varepsilon^0:D_0^2\overline{w}_0+\left(\omega_{SDT}^{Lin}\right)^2\overline{w}_0=0 \tag{33}$$

$$\varepsilon^1:D_0^2\overline{w}_1+\left(\omega_{SDT}^{Lin}\right)^2\overline{w}_1=-2D_0D_1\overline{w}_0-\lambda_{10}\overline{w}_0^2 \tag{34}$$

$$\begin{aligned} \varepsilon^2:\ &D_0^2\overline{w}_2+\Omega_0^2\overline{w}_2=-2D_0D_1\overline{w}_1-2D_0D_2\overline{w}_0-D_1^2\overline{w}_0-2\overline{\xi}_1D_0\overline{w}_0\\ &-2\overline{\theta}_1\overline{w}_0\overline{w}_1-\overline{\theta}_2\overline{w}_0^3+\overline{q}_0\cos(\omega_{SDT}^{Lin}\tau_0+\vartheta\tau_2) \end{aligned} \tag{35}$$

Solving Eqs. (33) and (34), yields the following expressions for $\overline{w}_0$ and $\overline{w}_1$:

$$\overline{w}_0=A(\tau_1,\tau_2)e^{i\omega_{SDT}^{Lin}\tau_0}+\overline{A}(\tau_1,\tau_2)e^{-i\omega_{SDT}^{Lin}\tau_0} \tag{36}$$

$$\overline{w}_1=\frac{\overline{\theta}_1}{\left(\omega_{SDT}^{Lin}\right)^2}\left(-2A(\tau_2)\overline{A}(\tau_2)+\frac{1}{3}A^2(\tau_2)e^{2i\omega_{SDT}^{Lin}\tau_0}+\frac{1}{3}A^2(\tau_2)e^{-2i\omega_{SDT}^{Lin}\tau_0}\right) \tag{37}$$

where $A(\tau_1,\tau_2)$ and $\overline{A}(\tau_1,\tau_2)$ indicate unknown complex and conjugate functions. It should be emphasized that while $\overline{w}_1$ is being found, it is taken into account that $\frac{\partial A(\tau_1,\tau_2)}{\partial\tau_1}=0$.

Substituting the expressions (36) and (37) for $\overline{w}_0$ and $\overline{w}_1$ in Eq. (35), the secular terms are set to zero:

$$2i\omega_{SDT}^{Lin}\left(\frac{\partial A(\tau_2)}{\partial \tau_2}+\overline{\xi}_1 A(\tau_2)\right)+\left(3\overline{\theta}_2-\frac{10\overline{\theta}_1^2}{3\left(\omega_{SDT}^{Lin}\right)^2}\right)A^2(\tau_2)\overline{A}(\tau_2)$$
$$-0.5\overline{q}_0 e^{i\vartheta\tau_2}=0 \tag{38}$$

The solution of Eq. (38) is sought in polar coordinates as follows:

$$A(\tau_2)=0.5r(\tau_2)e^{i\phi(\tau_2)} \tag{39}$$

where $r(\tau_2)$ and $\varphi(\tau_2)$ denote amplitude and phase of vibration.

By replacing (39) into (38), the following equations are obtained when the real and imaginary parts are set to zero separately:

$$\frac{\partial r}{\partial \tau_2}=-\overline{\xi}_1 r+\frac{\overline{q}_0}{2\omega_{SDT}^{Lin}}\sin\psi \tag{40}$$

$$\frac{\partial \psi}{\partial \tau_2}=\vartheta-\frac{9\overline{\theta}_2\left(\omega_{SDT}^{Lin}\right)^2-10\overline{\theta}_1^2}{24\left(\omega_{SDT}^{Lin}\right)^3}r^2+\frac{\overline{q}_0}{2r\omega_{SDT}^{Lin}}\cos\psi \tag{41}$$

where $\psi=\vartheta\tau_2-\phi$ denotes the new phase angle.

From the conditions $\frac{\partial \psi}{\partial \tau_2}=0$ and $\frac{\partial r}{\partial \tau_2}=0$, in the presence of steady-state motions, the following expression for the detuning parameter is obtained:

$$\vartheta_{1,2}=\upsilon f^2\pm\left(\frac{\overline{q}_{01}^2}{4\left(\omega_{SDT}^{Lin}\right)^2 f^2}-\overline{\xi}_1^2\right)^{0.5} \tag{42}$$

where

$$\upsilon=\frac{h^2}{8\omega_{SDT}^{Lin}}\left(3\overline{\theta}_2-\frac{10\overline{\theta}_1^2}{3\left(\omega_{SDT}^{Lin}\right)^2}\right),\ \overline{q}_{01}^2=\frac{\overline{q}_0^2}{h^2},\ f=\frac{r}{h} \tag{43}$$

Substituting expression (42) into (32), the damped nonlinear forced vibration frequency–amplitude dependence for NHO shell-type structural elements with a double curvature at primary resonance in the framework of SDT, we obtain:

$$\Omega_{SDT}^{NLforc_i}=\omega_{SDT}^{Lin}+\varepsilon^2\left\{\upsilon f^2\pm\left(\frac{\overline{q}_{01}^2}{4\left(\omega_{SDT}^{Lin}\right)^2 f^2}-\overline{\xi}_1^2\right)^{0.5}\right\},(i=1,2) \tag{44}$$

Here, the plus sign corresponds to the non-linear forced-1 (abbreviated $forc_1$) frequency component, and the negative sign corresponds to the non-linear forced-2 (abbreviated $forc_2$) frequency component.

From the expression (44), the ratio of the nonlinear forced frequency to the linear frequency with damping is easily found as:

$$\frac{\Omega_{SDT}^{NLforc_i}}{\omega_{SDT}^{Lin}}=1+\frac{\varepsilon^2}{\omega_{SDT}^{Lin}}\left\{\upsilon f^2\pm\left(\frac{\overline{q}_{01}^2}{4\left(\omega_{SDT}^{Lin}\right)^2 f^2}-\overline{\xi}_1^2\right)^{0.5}\right\}(i=1,2) \tag{45}$$

The dependences (44) and (45) can be used for NHO shell-type structural elements such as spherical and hypar shells, panels and plates with viscous damping in the framework of SDT, as $R_1=R_2$, $R_2=-R_1$, $R_1\to\infty$ and $R_1\to\infty$, $R_2\to\infty$, respectively (see, Fig. 2a–2d).

In a particular case, the frequency of nonlinear forced vibrations and the ratio of nonlinear forced vibrations to the linear frequency for NHO structures without damping in the scope of SDT can be found from dependences (44) and (45), at $\xi=0$

In a particular case, the backbone curve associated with undamped free vibrations (Ω_{SDT}^{NLbb}) for NHO shell-type structural elements with a double curvature within SDT can be found from expression (44), when $q_0=0$ and $\xi=0$.

Dependences (44) and (45) can be used in the framework of CST, as the influences of transverse shear deformations are not considered into account in basic relationships. In this case, the symbols use CST instead of SDT.

Table 1
Comparison the $\Omega_{CST}^{NLbb}/\omega_{CST}^{Lin}$ ratio for HO cylindrical shell within CST with the Ref. [19].

f	Sheng and Wang [19]	Present study
0.5	1.0017	1.00185
1.0	1.0066	1.0741
1.5	1.0149	1.0166
2.0	1.0265	1.0296
2.5	1.0414	1.0463

Table 2
Comparison the linear vibration frequencies of homogeneous plates with various orthotropy ratios in the framework of SDT with the results of Thai and Kim [30].

l_1/l_2	$E_{11}^0/E_{22}^0\to l_1/h$	Thai and Kim [30]		Present study	
		10	20	10	20
		$\hat{\omega}_{SDT}^{Lin}$			
0.5	10	8.5241	11.0551	8.5282	10.9871
	20	9.1141	12.4009	9.1168	12.3802
1.0	10	9.5628	11.9334	9.5668	11.7472
	20	10.2349	13.2676	10.2379	13.2029
2.0	10	14.9934	16.4739	15.1724	16.4735
	20	16.5030	18.4742	16.5746	18.4795

4. Numerical applications

Firstly, the accuracy of present formulas is confirmed by comparisons and then numerical analyzes on the $\Omega_{SDT}^{NLforc_i}$ and $\Omega_{SDT}^{NLforc_i}/\omega_{SDT}^{Lin}$ $(i=1,2)$ for NHO shell-type structural members are presented in comparison with the appropriate results obtained in the framework of classical shell theory.

In order to verify the present results, $\Omega_{CST}^{NLbb}/\omega_{CST}^{Lin}$ for HO cylindrical shell within CST are compared with Ref. [19] and presented in Table 1. The nonlinear backbone frequency Ω_{CST}^{NLbb} is obtained by writing $\xi=0$, $q_0=0$ and $\eta_i=1(i=1,2)$ in (42), when the influences of transverse shear deformations are not considered. The following parameters are used for the comparison: $l_1=0.4, l_2=1.5748R_2, R_1\to\infty$, $R_2=100$ h, $E_{11}^0=2\times10^{11}$ Pa, $E_{22}^0=G_{12}^0=E_{11}^0/20$, $\nu_{12}=0.2$, and $\rho_0=7800$ kg/m^3. It should be emphasized that at $R_2/h=100$, the $\Omega^{NLbb}/\omega^{Lin}$ ratios within the CST and SDT are approximately the same. The comparison of the magnitudes for $\Omega_{CST}^{NLbb}/\omega_{CST}^{Lin}$ ratio, which are presented in Ref. [19], with the magnitudes obtained for a particular case in our study, shows that the results are in good agreement (see, Table 1).

In the second comparison, the results obtained in the study of Thai and Kim [30] for linear vibration frequencies of HO plates with various orthotropy ratios in the framework of SDT are compared with our results. Considering $\mu_1=0, R_1\to\infty$, $R_2\to\infty$ in the expression (24) in our study, the expression for linear vibration frequencies of HO plates is obtained in the framework of SDT. In the comparison, the E_{11}^0/E_{22}^0 ratio changes and the other HO material properties are as follows: $G_{12}^0/E_{22}^0=G_{13}^0/E_{22}^0=0.5$, $G_{23}^0/E_{22}^0=0.2, \nu_{12}=0.25, \rho^0=1$. The variation of geometric parameters is shown in Table 2. The following formula is used for the nondimensional frequency in a comparison: $\hat{\omega}_{SDT}^{Lin}=\omega\frac{l_1}{h}\sqrt{\frac{\rho^0}{E_{22}^0}}$. The very good agreement of the obtained results confirms the accuracy of the expression obtained for the frequency in the framework of SDT in our study (see, Table 2).

In numerical analysis, various shell-type structural elements made of graphite/epoxy with the following material properties are used (except for Figs. 5 and 6) [11]:

$$E_{11}^0=137.9\text{ GPa},\ E_{22}^0=8.96\text{ GPa},\ G_{12}^0=G_{13}^0=7.1\text{ GPa},$$
$$G_{23}^0=6.21\text{ GPa},\ \nu_{12}=0.3, \nu_{21}=\nu_{12}E_{22}^0/E_{11}^0,$$
$$\rho^0=1.45\times10^3\ (\text{kg/m}^3)$$

The non-homogeneity functions vary exponentially as follows: $\eta_i(\overline{z})=e^{\mu_i(\overline{z}+1/2)}(i=1,2)$, where $\mu_i(i=1,2)$ are the coefficients of variation

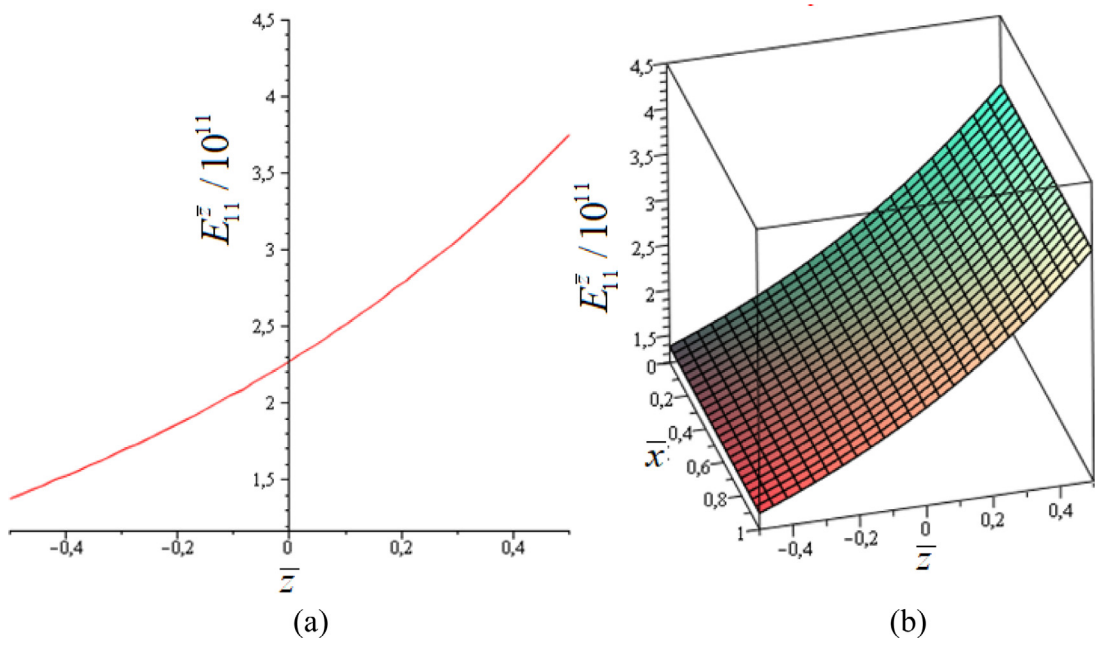

Fig. 4. (a) Two- and (b) three-dimensional distributions of Young's modulus ($E_{11}^{\bar{z}}$).

of elasticity moduli and density, those vary in the range of $0 \le \mu_i \le 1$, while the case of $\mu_i = 0$ corresponds to HO material. By using Maple 14, (a)two- and (b) three-dimensional distributions of the Young's modulus ($E_{11}^{\bar{z}}$) are illustrated in Fig. 4. Here $\bar{x} = x/l_1$ is the dimensionless longitudinal coordinate. Variations of other mechanical properties with respect to the thickness coordinate can be plotted similarly

The nonhomogeneity types of material properties of shell-type structural elements are designated by symbols as follows: $(\mu_1, \mu_2) = (1, 0)$ or NHO-1 and $(\mu_1, \mu_2) = (+1, +1)$or NHO-2. The damping coefficient is taken into account as $\xi = \xi_1 \omega^{Lin}$ [19,31]. In all calculations and analyzes performed below, the main vibrational mode $(m, n) = (1, 1)$ has been considered.

The variations of damped and undamped nonlinear forced vibration frequencies and undamped backbone frequency of HO and NH orthotropic (NHO-1) spherical shell and hypar shell against the f within (a) shear and (b) classical theories are illustrated in Figs. 5 and 6 for different orthotropy ratios $E_{11}^0/E_{22}^0 = 10, 15, 20$. The other parameters are taken into account: $G_{12}^0/E_{22}^0 = G_{13}^0/E_{22}^0 = 0.5$, $G_{23}^0/E_{22}^0 = 0.2$, $\nu_{12} = 0.25$, $\rho^0 = 1$, $R_2/l_1 = 3$, $l_1/l_2 = 1$, $l_1/h = 10$, $q_0 = 1.388 \times 10^7$ (Pa/m), $\xi_1 = 0$ and $\xi_1 = 0.05$. As shown in Figs. 5 and 6, due to the rise of f, Ω^{NLforc_2} and Ω^{NLbb} of shallow shells with and without damping increment, while Ω^{NLforc_1} first reduces and then increment. The damped and undamped nonlinear forced vibration frequencies and *backbone* frequency of shallow shells reduce due to E_{11}^0/E_{22}^0 increment from 10 to 20. The undamped nonlinear forced vibration frequencies and backbone frequency of spherical shells are more significant than those of hypar shells at $f > 0.8$. The nonlinear forced vibration and *backbone* frequencies of hypar shells are less than those of spherical shells when the viscous damping is taken into account. Due to the increase of f, the effect of shear deformations on the Ω^{NLforc_2} and Ω^{NLbb} for shallow shells without damping decreases, while it first raises to its maximum value and then diminishes for the $forc_1$ frequency. For example, due to the rise of f from 0.16 to 1.60 at $E_{11}^0/E_{22}^0 = 20$, the influence of shear deformations on the Ω^{NLforc_2} and Ω^{NLbb} for spherical shells originating from NHO-1 decreases (12.36%) and (5.98%), respectively. At the same time, it first increases by (2.29%) and then diminishes by (3.97%) for the Ω^{NLforc_1}. The effect of shear deformations on Ω^{NLforc_2} and Ω^{NLbb} for the hypar shell originating from NHO-1 diminishes (18.32%) and (10.57%), respectively, while it first rises by (2.2%) and then reduces by (7.69%) for the Ω^{NLforc_1} for hypar shells. The influence of shear deformations on damped and undamped nonlinear forced vibration frequencies and *backbone* frequency of shallow shells originating from NHO-1 rises due to the orthotropy ratio increment. For example, due to the rise of E_{11}^0/E_{22}^0 from 10 to 20 at $f = 0.16$, the effect of transverse shear deformations on Ω^{NLforc_1}, Ω^{NLforc_2} and Ω^{NLbb} for NHO-1 originating spherical and hypar shells with and without damping increase (3.5%), (9.8%), (6%) and (3.4%), (10.2%), (6.1%), respectively.

Due to the increase of the E_{11}^0/E_{22}^0 ratio, the effect of the NHO-1 profile on the Ω^{NLforc_1} for shallow shells with and without viscous damping decreases, whereas it rises for Ω^{NLforc_2}. The effect of the NHO-1 profile on the *backbone* frequency of shallow shells remains constant. For example, due to the rise of E_{11}^0/E_{22}^0 from 10 to 20 at $f = 0.16$, the influence of the NHO-1 profile on the Ω^{NLforc_1} for spherical and hypar shells under SDT diminishes by (3.2%) and (2.8%), whereas raises by (13.9%) and (15.5%) for Ω^{NLforc_2}, respectively.

The viscous damping effect on forced vibration frequencies for shallow shells decreases as the orthotropy ratio increment. For example, as E_{11}^0/E_{22}^0 increment from 10 to 20, the influence of damping on nonlinear forced vibration frequencies for the spherical shell consisting of raw material diminishes (1%) and (1.8%) at $f = 0.8$, while it for NHO-1 profiles reduce (1%) and (1.1%) within SDT and CST, respectively at $f = 0.48$. Similarly, the damping influence on forced vibration frequencies of hyperbolic-paraboloid shells originating from raw material and NHO-1 material diminishes (0.6%) in the framework SDT and CST, at $f = 0.8$.

Figs. 7 and 8 show the variation of nonlinear forced vibration and *backbone* frequencies four different structural elements such as HO and NHO-1 spherical and hypar shells, cylindrical panels and plates depending on the increase of f for various damping coefficient ξ_1 within (a) SDT and (b) CST. The numerical data used in the drawing of Figs. 7 and 8 are as follows: $R_2/l_1 = 1, l_1/l_2 = 1, l_1/h = 20, q_0 = 1.0476 \times 10^7$, $\xi_1 = 0, 0.06, 0.07, 0.08$. While the Ω^{NLforc_1} and Ω^{NLbb} for spherical shell decrease, the Ω^{NLforc_2} first increases and then reduces with the increasing of f, as the damping coefficient is zero. While the Ω^{NLforc_1} and Ω^{NLbb} for the spherical shell with damping decrease depending on the increase of f, the Ω^{NLforc_2} increases. Due to the increase of f from 0.07 to 0.75, Ω^{NLforc_2} and Ω^{NLbb} increase for the

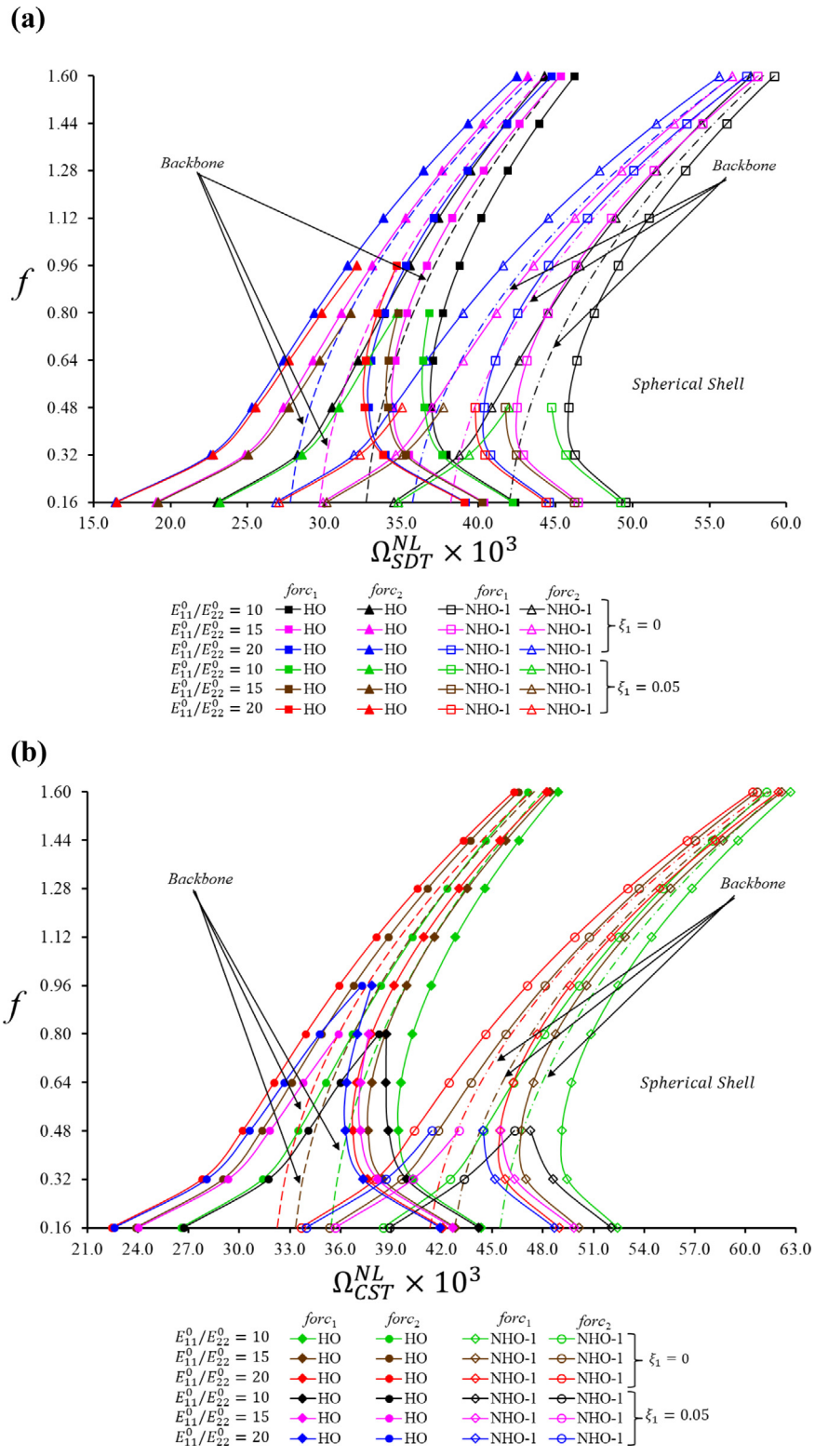

Fig. 5. Variation of nonlinear forced vibration frequencies of HO and NHO-1 spherical shells with and without damping against the f within (a) shear and (b) classical theories.

hypar shell, cylindrical panel and plate, in contrast, Ω^{NLforc_1} reduces to its minimum value and then raises, when damping is not taken into account. In the presence of damping, Ω^{NLforc_2} and Ω^{NLbb} increase, while the Ω^{NLforc_1} decreases, depending on the rise of f. For the all-structural elements, the undamped Ω^{NLforc_1} are larger than the undamped Ω^{NLforc_1}, and vice versa for Ω^{NLforc_2}. *Backbone* frequencies in undamped and damped cases are equal to each other.

The forced vibration and *backbone* frequencies of the spherical shell and the cylindrical panel are higher than the frequency of the plate, whereas those of hypar shell are less than the frequencies of the plate. Depending on the increase of damping parameter ξ_1, the difference

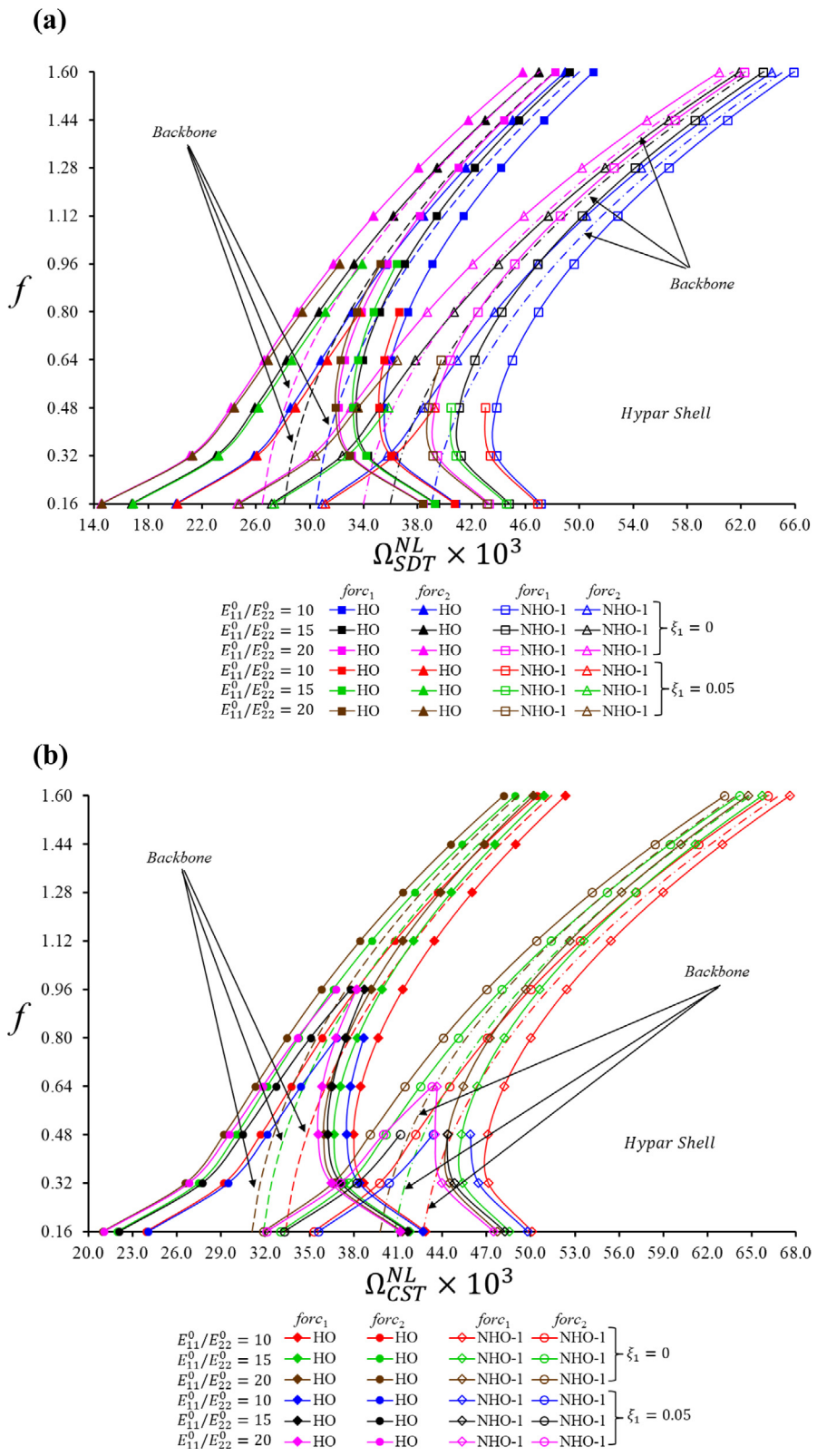

Fig. 6. Change of nonlinear forced vibration frequencies of HO and NHO-1 hyperbolic-paraboloid shells with and without damping against the f within (a) shear and (b) classical theories.

between Ω^{NLforc_1} decreases, while between Ω^{NLforc_2} increase in the spherical shell and cylindrical panel, while it remains constant in the hypar shell.

The influence of damping on nonlinear forced vibration frequencies of four structures increases with the increase of f. For example, due to the rise of f from 0.07 to 0.27 at $\xi_1 = 0.06$, the damping effect on the forced vibration frequencies of the HO- spherical shell increases

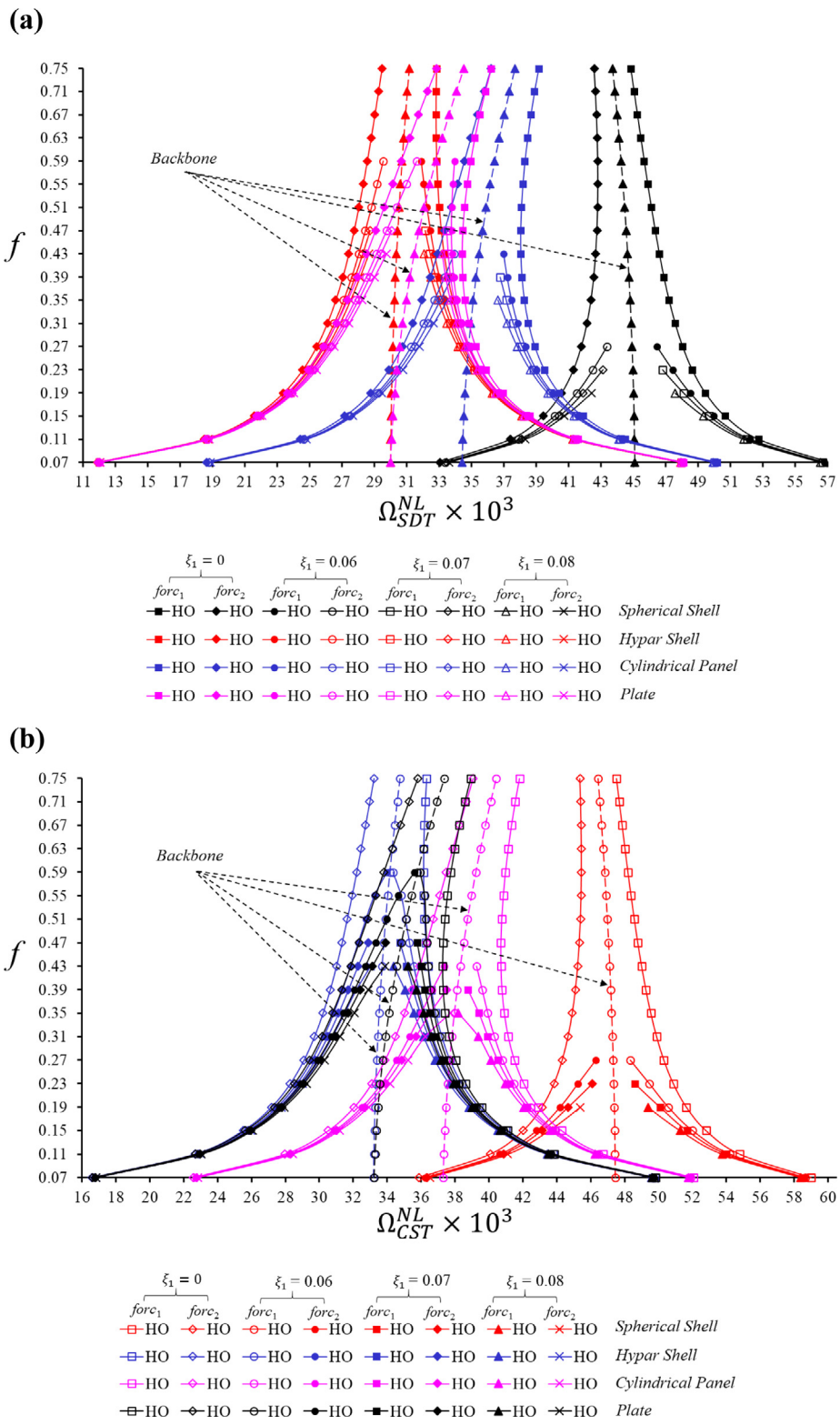

Fig. 7. Variation of nonlinear forced vibration frequencies of HO structures versus the f for various damping coefficient ξ_1 within (a) shear and (b) classical theories.

(2.8%) and (3.5%), while it increases (0.8%) and (1%) for the HO-hypar shell and HO-plate, (1.2%) and (1.4%) for the HO-cylindrical panel within shear and classical theories, respectively. The effect of damping on frequencies of structural elements increases depending on the rise of ξ_1. For instance, due to the increase of ξ_1 from 0.06 to 0.08 at $f = 0.11$, the influence of damping on the Ω^{NLforc_1} and Ω^{NLforc_2} for the spherical shell consisting of the NHO-1 profile within SDT raises (1.8%) and (2.19%), respectively. It rises (0.5%) and (0.8%) for Ω^{NLforc_1} and Ω^{NLforc_2} for the hyperbolic-paraboloid shell and plate, and it raises (0.7%) and (1.1%) for Ω^{NLforc_1} and Ω^{NLforc_2} for the cylindrical panel, respectively. The damping influence for CST is more pronounced

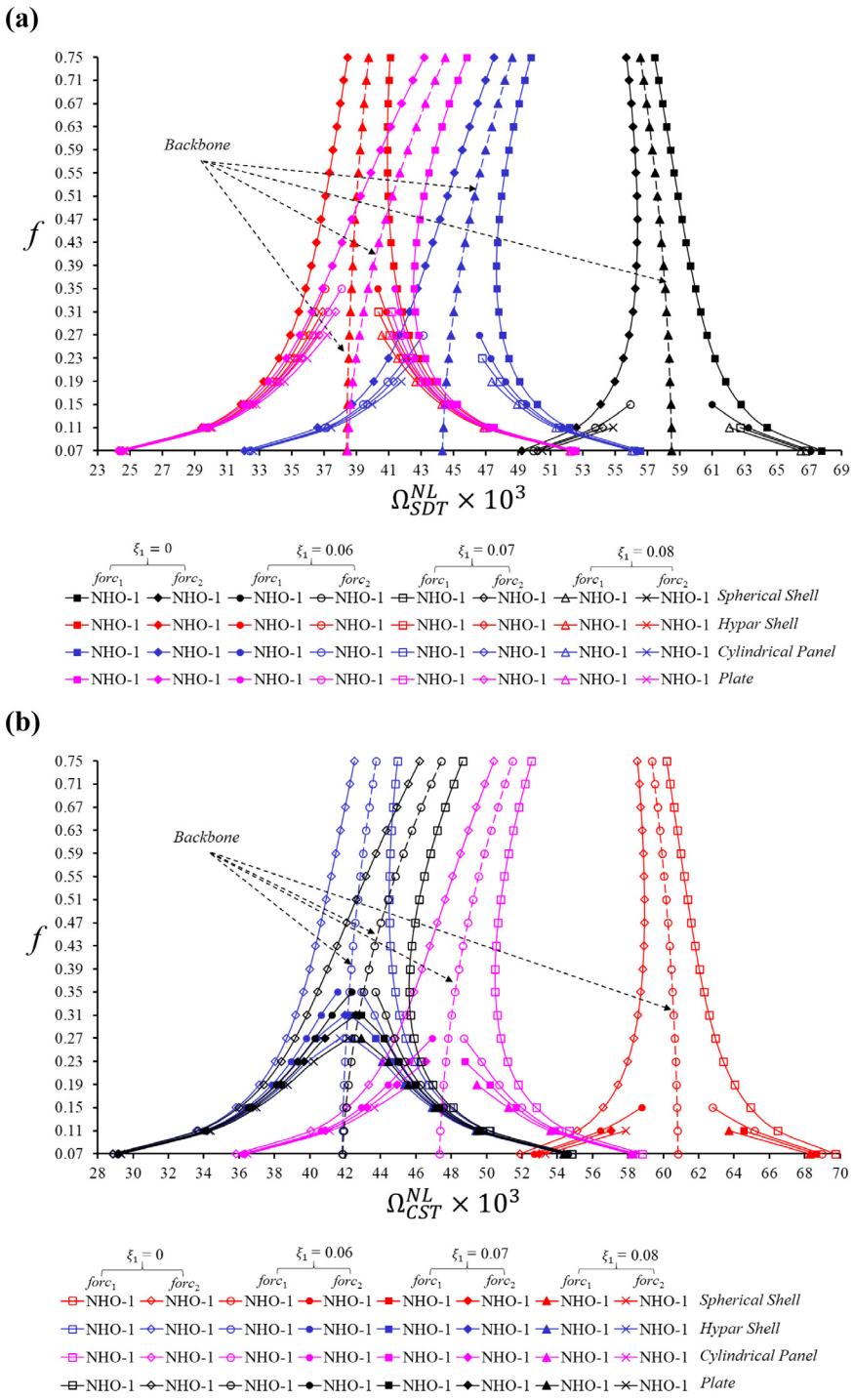

Fig. 8. Distribution of nonlinear forced vibration frequencies of NHO-1 structural members versus the f for various damping coefficient ξ_1 within (a) SDT and (b) CST.

by (0.4%) for the spherical shell and by (0.15%) for the hyperbolic-paraboloid shell, cylindrical panel, and plate than the damping effect in the SDT.

While the effect of the transverse shear deformations on the nonlinear forced vibration frequencies of structural elements decreases for Ω^{NLforc_1}, it raises for Ω^{NLforc_2} due to the increase of ξ_1. For example, as ξ_1 increment from 0 to 0.08, the change of the transverse shear deformations effect on forced frequencies for the NHO-1 structural elements such as for spherical shell is (0.6%) at $f = 0.11$, for the hypar shell and plate is (2.6%) at $f = 0.27$ and for the cylindrical panel is (1%) at $f = 0.19$.

While the effect of NHO-1 profile on the Ω^{NLforc_1} for structural elements decreases, it increases for Ω^{NLforc_2} due to the rise of ξ_1. For instance, due to the increase of ξ_1 from 0 to 0.08, the change of the NHO-1 profile effect on the Ω^{NLforc_1} and Ω^{NLforc_2} for the spherical shell is (2.8%) and (3.3%) at $f = 0.11$, for the hypar shell and plate it is (5.3%) and (6.1%) at $f = 0.27$ and for the cylindrical panel it is (3.1%) and (3.6%) at $f = 0.19$, respectively within CST. The effect of the NHO-1 profile on the forced frequencies in the SDT is lower than in the CST by (0.6%) for a spherical shell and (0.2%) for a hypar shell, cylindrical panel and plate.

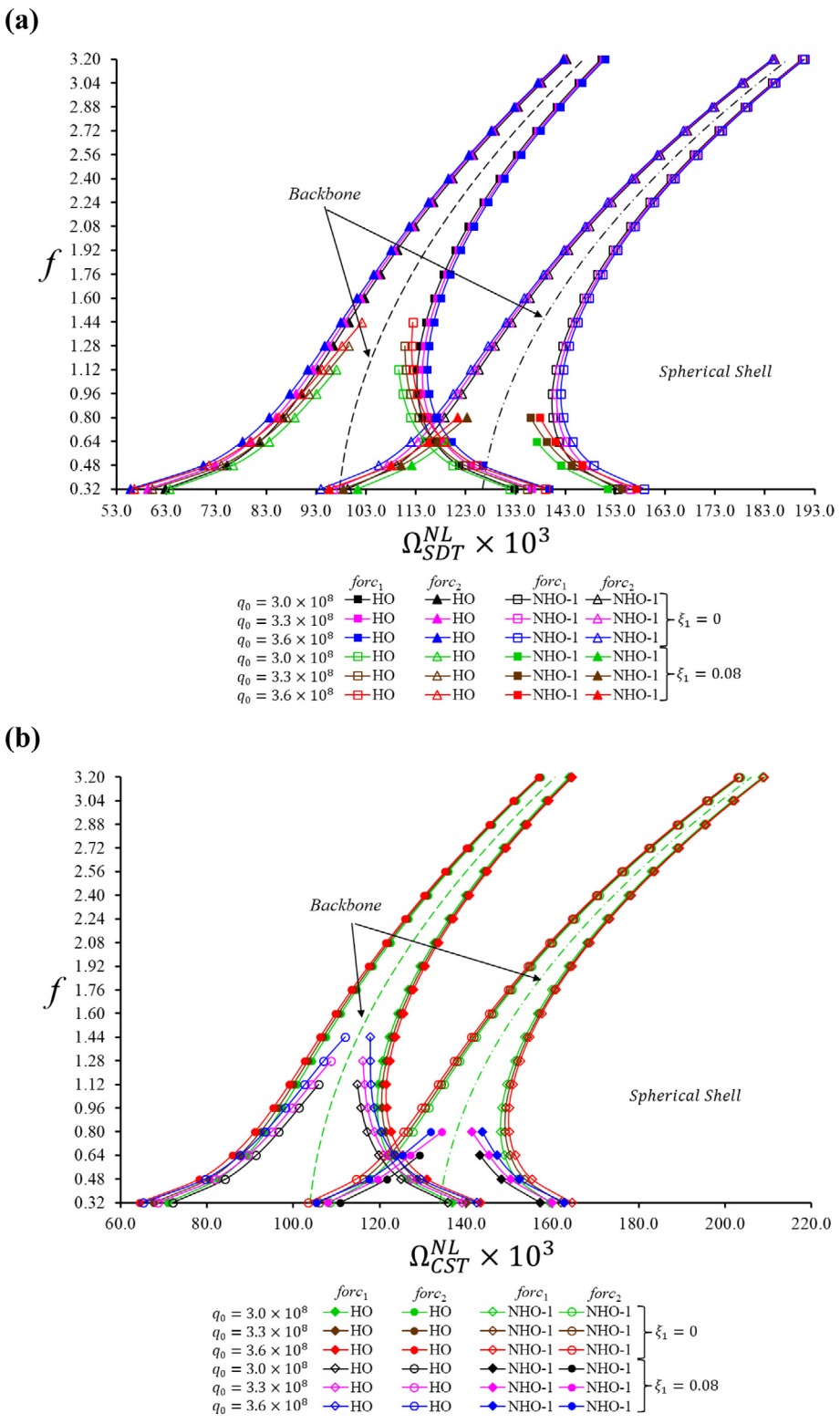

Fig. 9. Variation of undamped/damped nonlinear forced vibration frequencies of HO and NHO-1 spherical shells versus f for different q_0 within (a) shear and (b) classical theories.

Figs. 9 and 10 show the change of the undamped/damped nonlinear forced vibration and *backbone* frequencies of HO and NHO-1 orthotropic spherical and hyperbolic-paraboloid shells depending on the amplitude of f for various q_0 within (a) SDT and (b) CST. The following loading, damping and geometric parameters are used: $q_0 = 3 \times 10^8, 3.3 \times 10^8, 3.6 \times 10^8$, $R_2/l_1 = 1, l_1/l_2 = 3, l_1/h = 10$, $\xi_1 = 0$ and $\xi_1 = 0.08$. As shown in Figs. 9 and 10, depending on the increase of f, the undamped and damped Ω^{NLforc_1} and Ω^{NLbb} for shallow shells raise, while the undamped and damped Ω^{NLforc_2} it first reduces to its minimum value and then raises. As the undamped and damped Ω^{NLforc_1} of the shells increase due to increment of q_0, whereas the Ω^{NLforc_2} diminish. The undamped forced vibration frequencies of the

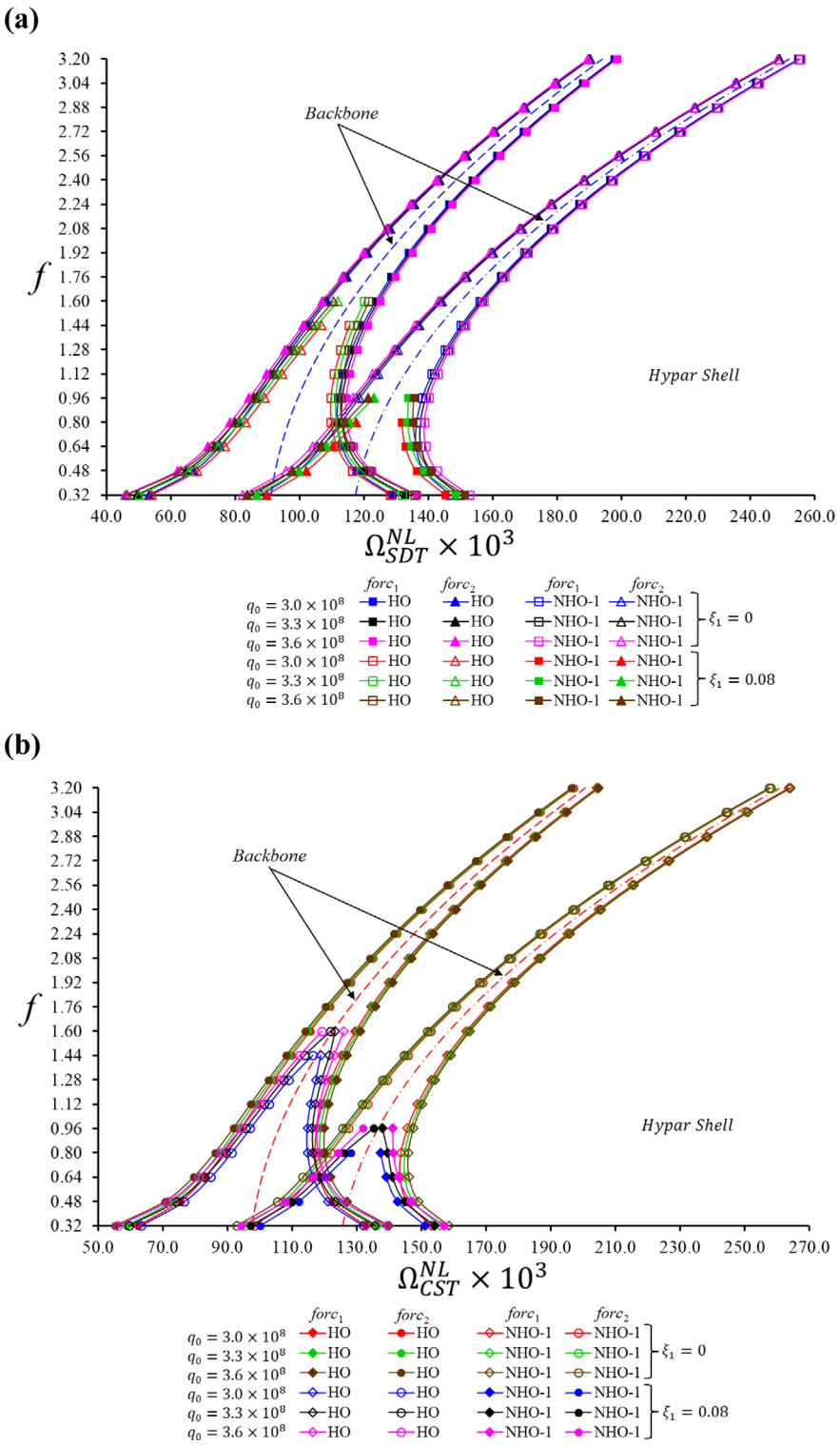

Fig. 10. Variation of undamped/damped nonlinear forced vibration frequencies of HO and NHO-1 hyperbolic-paraboloid shells versus f for different q_0 within (a) shear and (b) classical theories.

hyperbolic-paraboloid shell are more pronounced than the undamped forced vibration frequencies for the spherical shell, at $f > 1.12$, vice versa in the damped case.

Due to the increase of f from 0.32 to 3.2, the effect of shear deformations on the undamped Ω^{NLforc_1} and Ω^{NLbb} for the spherical shell raises, while it first reduces to its minimum value and then raises for the undamped Ω^{NLforc_2}. While the influence of shear deformations on the undamped Ω^{NLforc_2} and Ω^{NLbb} for hyperbolic-paraboloid shell diminishes, it first increases to its maximum value and then reduces for undamped Ω^{NLforc_1}. The influence of shear deformations on Ω^{NLforc_1} for shallow shells in the undamped and damped cases diminish, at the same time, it raises for Ω^{NLforc_2}, when q_0 increases for fixed f. As the q_0 increases from 3×10^8 to 3.6×10^8, the effect of shear deformations on the undamped and damped Ω^{NLforc_2} for HO-spherical and HO-

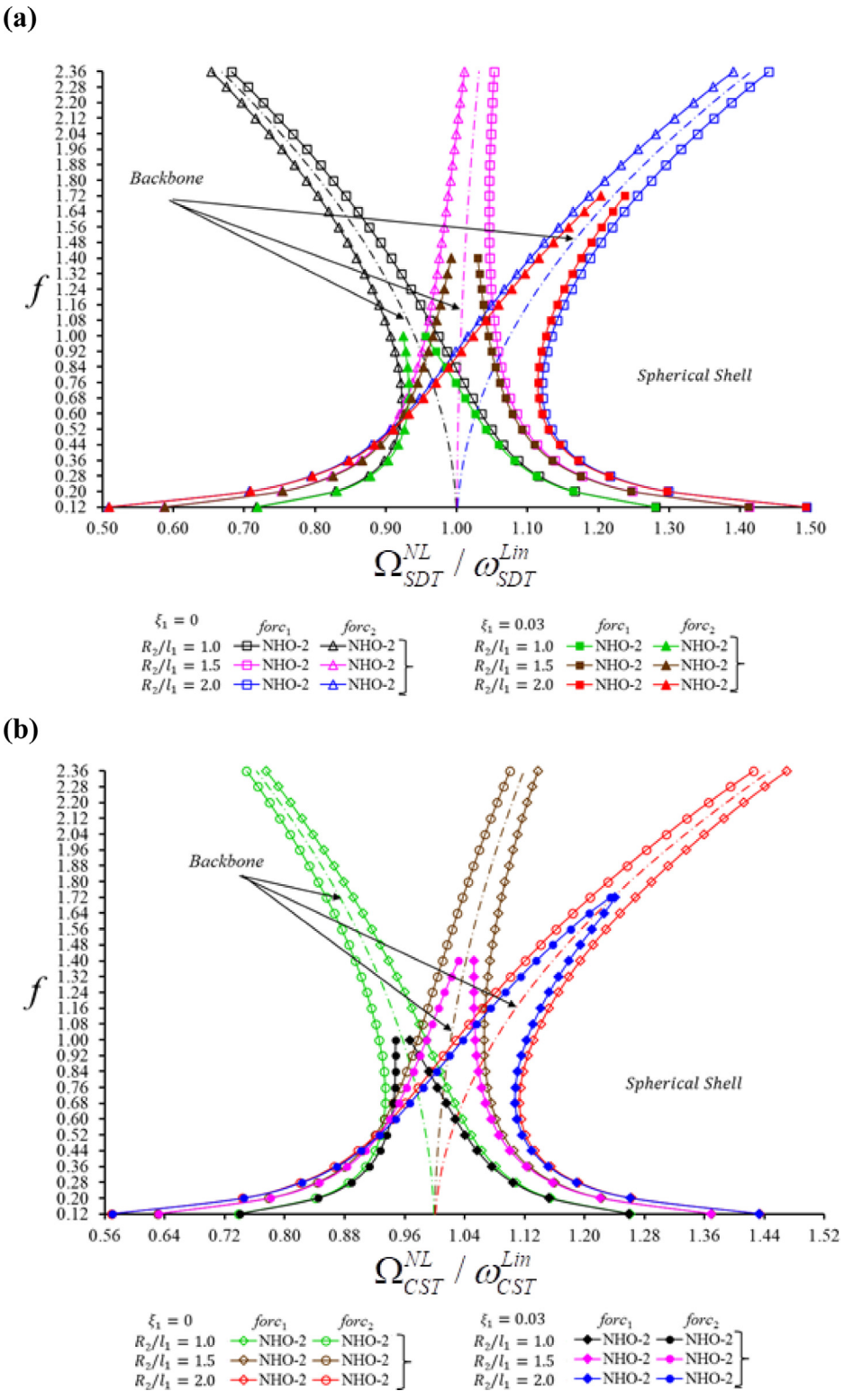

Fig. 11. Distribution of undamped/damped nonlinear forced vibration frequencies to linear frequency ratios of NHO-2 spherical shells versus f for different R_2/l_1 within (a) SDT and (b) CST.

hyperbolic-paraboloid shells increases (1.8%) and (2.8%), respectively, whereas, it for Ω^{NLforc_1} is less than (0.5%) at $f = 0.32$.

Due to the increase of q_0 from 3×10^8 to 3.6×10^8, the effect of NHO-1 profile on the Ω^{NLforc_1} for spherical and hypar shells in the undamped and damped cases within CST diminishes by (1.8%) and (1.9%), respectively, whereas it raises by (%7.5) and (%10) for the Ω^{NLforc_2} frequencies, at $f = 0.32$.

The damping effect on nonlinear forced vibration frequencies of shallow shells diminishes due to the rise of q_0 from 3×10^8 to 3.6×10^8. For instance, due to the increase of q_0 from 3×10^8 to 3.6×10^8 at $f =$

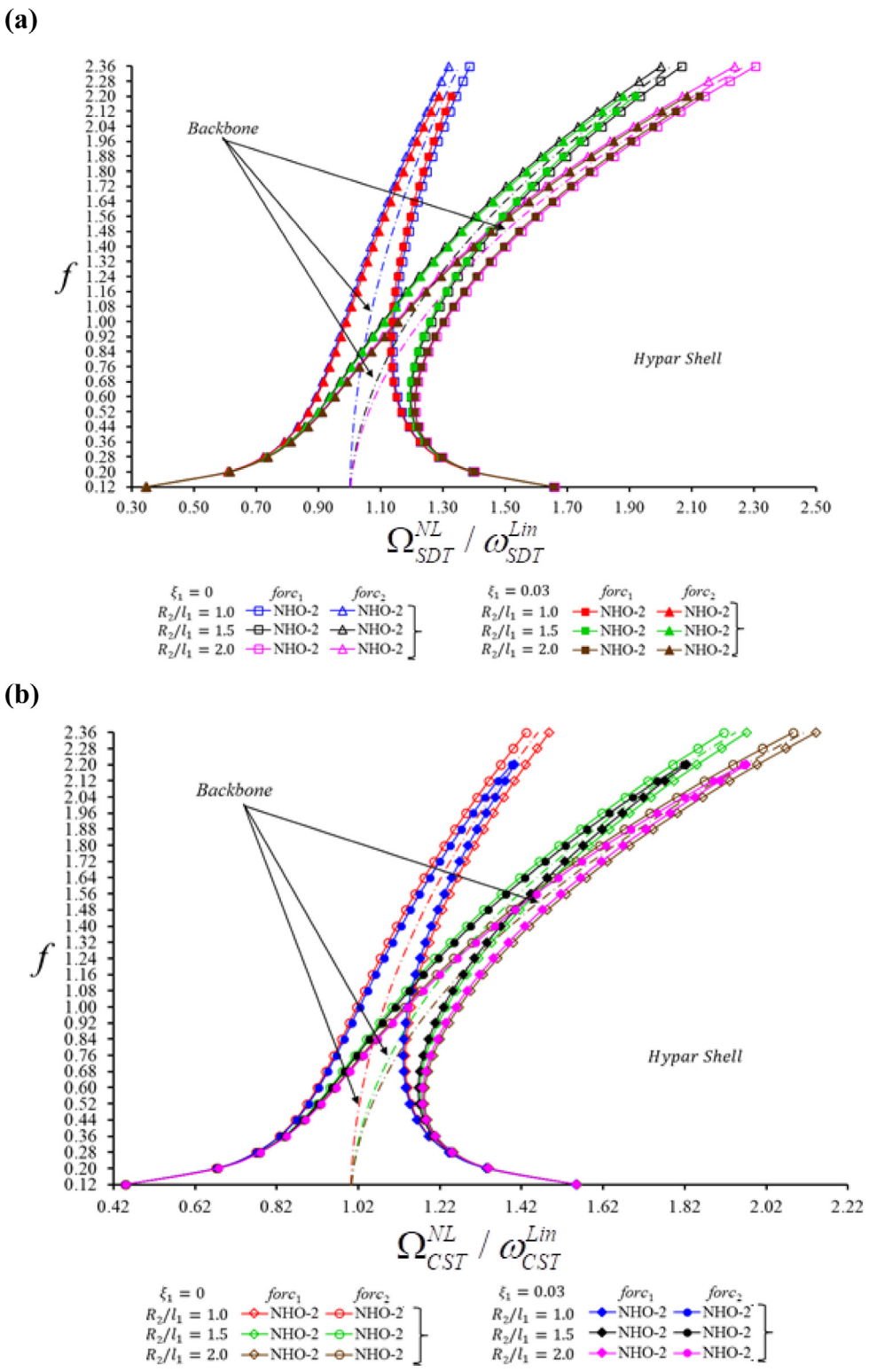

Fig. 12. Distribution of undamped/damped nonlinear forced vibration frequencies to linear frequency ratios of NHO-2 hypar shells versus f for different R_2/l_1 within (a) shear and (b) classical theories.

1.12, the damping effect on the nonlinear forced vibration frequencies of the spherical shell consisting of the HO profile decreases (0.85%) and (1.2%), while this influence for the HO- hyperbolic-paraboloid shell diminishes (0.6%) and (1.7%) within shear and classical theories, respectively.

In Figs. 11 and 12 are presented the variation of nonlinear forced vibration frequency to linear frequency ratios of the NHO-2 spherical and hypar shells with and without damping within two shell theories versus f for different R_2/l_1 ratio. The following data is used for the calculations: $R_2/l_1 = 1, 1.5, 2, l_1/l_2 = 1, l_1/h = 10, q_0 = 3.2 \times 10^7$, $\xi_1 = 0$ and $\xi_1 = 0.03$. Due to the increase of f, the undamped

and damped $\Omega^{NLforc_2}/\omega^{Lin}$ and $\Omega^{NLbb}/\omega^{Lin}$ ratios rise, whereas the $\Omega^{NLforc_1}/\omega^{Lin}$ ratio first reduces to its minimum value and then raises for the hypar shell. Undamped $\Omega^{NLforc_1}/\omega^{Lin}$ and $\Omega^{NLbb}/\omega^{Lin}$ ratios for spherical shell diminish, whereas $\Omega^{NLforc_2}/\omega^{Lin}$ ratio first increases to its maximum value and then decreases, as f increment at $R_2/l_1 = 1$,. Due to the increase of f, as $R_2/l_1 > 1$, the undamped and damped $\Omega^{NLforc_2}/\omega^{Lin}$ and $\Omega^{NLbb}/\omega^{Lin}$ ratios of the spherical shell rise, while the $\Omega^{NLforc_1}/\omega^{Lin}$ frequency ratio first diminishes and then increment. Due to the rise of the R_2/l_1 ratio from 1 to 2, the undamped and damped $\Omega^{NLforc_1}/\omega^{Lin}$ and $\Omega^{NLbb}/\omega^{Lin}$ ratios of spherical shells decrease, while $\Omega^{NLforc_2}/\omega^{Lin}$ ratio first diminishes to its minimum value and then increases. The undamped and damped forced vibration and *backbone* frequency ratios of the hyperbolic-paraboloid shell raise.

Depending on the increase of f, the effect of shear deformations on the undamped and damped forced vibration frequency ratios for shallow shells first diminishes to its minimum value and then increases, at the same time, this effect on the *backbone* frequency ratios rises for fixed R_2/l_1. For example, due to the increase of f from 0.12 to 2.36 at $R_2/l_1 = 1$, the influence of shear deformations on the undamped $\Omega^{NLforc_1}/\omega^{Lin}$ and $\Omega^{NLforc_2}/\omega^{Lin}$ ratios of the spherical shell firstly diminishes by (1.64%) and (1.95%) then rise by (11.94%) and (11.79%), respectively. Also, the shear deformations effect on the undamped *backbone* frequency ratio raises by (12.3%). The shear deformation influence on the undamped $\Omega^{NLforc_1}/\omega^{Lin}$ and $\Omega^{NLforc_2}/\omega^{Lin}$ ratios of the hypar shell firstly decrease by (6.56%) and (20.2%) then increase by (6.68%) and (5%), respectively. Besides, the shear deformation effect on the *backbone* frequency ratio rises by (7.2%). When $R_2/l_1 = 1.5$ and $f = 1.4$, the influence of shear deformations on the undamped and damped $\Omega^{NLforc_1}/\omega^{Lin}$ ratios of the spherical shell is (2.5%) and (2.1%), respectively. At the same time, this effect on the undamped and damped $\Omega^{NLforc_2}/\omega^{Lin}$ ratios are (3.4%) and (3.8%), respectively.

Due to the increase of R_2/l_1 from 1 to 2, the shear deformations effect on undamped and damped forced vibration frequency ratios of the spherical shell raises in the range of $0.12 \le f \le 0.68$, while it decreases at $f > 0.76$. The influence of shear deformations on the undamped and damped $\Omega^{NLforc_1}/\omega^{Lin}$ ratios of the hyperbolic-paraboloid shell rise, while it diminishes for the undamped and damped $\Omega^{NLforc_2}/\omega^{Lin}$ ratios. Due to the rise of R_2/l_1 from 1 to 2, the variation of the shear deformation effect on the undamped and damped *backbone* frequency ratios of shallow shells is insignificant. For instance, depending on the rise of R_2/l_1 ratio from 1 to 2 at $f = 0.12$, the effect of shear deformations on the undamped and damped $\Omega^{NLforc_1}/\omega^{Lin}$ and $\Omega^{NLforc_2}/\omega^{Lin}$ ratios of the spherical shell increment (2.6%) and (7.8%), respectively. Due to the increase of R_2/l_1 ratio from 1 to 2 at $f = 2.2$, the influence of shear deformations on undamped and damped $\Omega^{NLforc_1}/\omega^{Lin}$ ratios for the hypar shell raises (1.12%) and (2.5%) respectively. At the same time, it diminishes (0.4%) and (1.6%) for the undamped and damped $\Omega^{NLforc_2}/\omega^{Lin}$ ratios, respectively.

Due to the rise of f from 0.12 to 1.0, when $R_2/l_1 = 1$, the damping effect on $\Omega^{NLforc_i}/\omega^{Lin}$ for the spherical shell raises (1.7%) and (2.03%), whereas this effect in the hypar shells raises (0.6%) within shear and classical theories, respectively. The damping influence on forced frequency ratios for the shallow shell decreases with increasing of the R_2/l_1 ratio from 1 to 2. For instance, due to the increase of the R_2/l_1 ratio from 1 to 2 at $f = 1$, the effect of damping on $\Omega^{NLforc_2}/\omega^{Lin}$ for shallow shells diminishes about (1.1%) and (0.2%), respectively.

5. Conclusions

The damped nonlinear forced vibration behaviors of NHO structural elements at primary resonance in the framework of SDT is investigated. After mathematically modeling the mechanical properties of double curved structural systems composed of NHO materials, the nonlinear basic partial differential equations are derived based on nonlinear fundamental relationships. In the next step, these equations were reduced to ordinary differential equations containing second and third order nonlinearities with the Galerkin procedure, and the forced vibration frequency–amplitude dependence in the main resonance is found by solving them with the multi-scale method. After testing the correctness of the proposed methodology, the effects of inhomogeneity, transverse shear deformations, anisotropy and damping on the nonlinear forced vibration frequencies for various structural elements are investigated in detail, both qualitatively and quantitatively.

CRediT authorship contribution statement

A.H. Sofiyev: Conceptualization, Methodology, Formal analysis, Writing – original draft. **F. Turan:** Formal analysis, Writing – review & editing. **N. Kuruoğlu:** Writing – review & editing.

Declaration of competing interest

The authors declare that they have no known competing financial interests or personal relationships that could have appeared to influence the work reported in this paper.

Appendix A

$$
\begin{aligned}
&L_{11}(\varphi) = h\left[(A_{11}-A_{31})\frac{\partial^4}{\partial x^2\partial y^2} + A_{12}\frac{\partial^4}{\partial x^4}\right],\\
&L_{12}(w) = \rho_1\frac{\partial^4}{\partial x^2\partial\tau^2} - A_{13}\frac{\partial^4}{\partial x^4} - \left(A_{14}+A_{32}\right)\frac{\partial^4}{\partial x^2\partial y^2},\\
&L_{13}(\chi_1) = A_{15}\frac{\partial^3}{\partial x^3} + A_{35}\frac{\partial^3}{\partial x\partial y^2} - I_3\frac{\partial}{\partial x} - \rho_2\frac{\partial^3}{\partial x\partial\tau^2},\\
&L_{14}(\chi_2) = \left(A_{18}+A_{38}\right)\frac{\partial^3}{\partial x^2\partial y},\\
&L_{21}(\varphi) = h\left[A_{21}\frac{\partial^4}{\partial y^4} + (A_{22}-A_{31})\frac{\partial^4}{\partial x^2\partial y^2}\right],\\
&L_{22}(w) = -\left(A_{32}+A_{23}\right)\frac{\partial^4}{\partial x^2\partial y^2} - A_{24}\frac{\partial^4}{\partial y^4} + \rho_1\frac{\partial^4}{\partial x^2\partial\tau^2},\\
&L_{23}(\chi_1) = \left(A_{35}+A_{25}\right)\frac{\partial^3}{\partial x\partial y^2},\\
&L_{24}(\chi_2) = A_{38}\frac{\partial^3}{\partial x^2\partial y} + A_{28}\frac{\partial^3}{\partial y^3} - I_4\frac{\partial}{\partial y} - \rho_3\frac{\partial^3}{\partial y\partial\tau^2},\\
&L_{31}(\varphi) = h\left(\frac{1}{R_2}\frac{\partial^2}{\partial x^2} + \frac{1}{R_1}\frac{\partial^2}{\partial y^2}\right), L_{32}(u_3) = -\rho_t\frac{\partial^2}{\partial\tau^2},\ L_{33}(\psi_1) = I_3\frac{\partial}{\partial x},\\
&L_{34}(\chi_2) = I_4\frac{\partial}{\partial y},\ L_{35}(\varphi,w) = h\left[\frac{\partial^2}{\partial y^2}\frac{\partial^2}{\partial x^2} - 2\frac{\partial^2}{\partial x\partial y}\frac{\partial^2}{\partial x\partial y} + \frac{\partial^2}{\partial x^2}\frac{\partial^2}{\partial y^2}\right],\\
&L_{41}(\varphi) = h\left[B_{11}\frac{\partial^4}{\partial y^4} + (B_{12}+B_{21}+B_{31})\frac{\partial^4}{\partial x^2\partial y^2} + B_{22}\frac{\partial^4}{\partial x^4}\right],\\
&L_{42}(w) = -B_{23}\frac{\partial^4}{\partial x^4} - \left(B_{24}+B_{13}-B_{32}\right)\frac{\partial^4}{\partial x^2\partial y^2}\\
&\quad -B_{14}\frac{\partial^4}{\partial y^4} + \left(\frac{1}{R_2}\frac{\partial^2}{\partial x^2} + \frac{1}{R_1}\frac{\partial^2}{\partial y^2}\right),\\
&L_{43}(\chi_1) = B_{25}\frac{\partial^3}{\partial x^3} + \left(B_{15}+B_{35}\right)\frac{\partial^3}{\partial x\partial y^2},\\
&L_{44}(\chi_2) = \left(B_{28}+B_{38}\right)\frac{\partial^3}{\partial x^2\partial y} + B_{18}\frac{\partial^3}{\partial y^3},\\
&L_{45}(w,w) = -\left(\frac{\partial^2}{\partial x\partial y}\right)^2 + \frac{\partial^2}{\partial x^2}\frac{\partial^2}{\partial y^2}.
\end{aligned}
\tag{A.1}
$$

where

$$A_{11}=C_{111}B_{11}+C_{121}B_{21},\ A_{12}=C_{111}B_{12}+C_{121}B_{22},$$
$$A_{13}=C_{111}B_{13}+C_{121}B_{23}+C_{112},$$
$$A_{14}=C_{111}B_{14}+c_{121}B_{24}+c_{122},\ A_{15}=C_{111}B_{15}+C_{121}B_{25}+C_{151},$$
$$A_{18}=C_{111}B_{18}+C_{121}B_{28}+C_{181},$$
$$A_{21}=C_{211}B_{11}+C_{221}B_{21},\quad A_{22}=C_{211}B_{12}+C_{221}B_{22},$$
$$A_{23}=C_{211}B_{13}+C_{221}B_{23}+C_{212},$$
$$A_{24}=C_{211}B_{14}+C_{221}B_{24}+C_{222},\ A_{25}=C_{211}B_{15}+C_{221}B_{25}+C_{251},$$
$$A_{28}=C_{211}B_{18}+C_{221}B_{28}+C_{281},$$
$$A_{31}=C_{661}B_{35},\ A_{32}=C_{661}B_{32}+2C_{662},\quad A_{35}=C_{351}-C_{661}B_{35},$$
$$A_{38}=C_{381}-C_{661}B_{38},$$
$$I_k=\int_{-h/2}^{h/2}\frac{df_i^z}{dz}\mathrm{d}z,(i=1,2;\ k=i+2) \tag{A.2}$$

in which

$$B_{11}=\frac{C_{220}}{H},\ B_{12}=-\frac{C_{120}}{H},\ B_{13}=\frac{C_{120}C_{211}-C_{111}C_{220}}{H},$$
$$B_{14}=\frac{C_{120}C_{211}-C_{121}C_{220}}{H},$$
$$B_{15}=\frac{C_{250}C_{120}-C_{150}C_{220}}{H},B_{18}=\frac{C_{280}C_{120}-C_{180}C_{220}}{H},$$
$$B_{21}=-\frac{C_{210}}{H},\ B_{22}=\frac{C_{110}}{H},$$
$$B_{23}=\frac{C_{111}C_{210}-C_{211}C_{110}}{H},\ B_{24}=\frac{C_{121}C_{210}-C_{221}C_{110}}{H},$$
$$B_{25}=\frac{C_{150}C_{210}-C_{250}C_{110}}{H},\ B_{31}=\frac{1}{C_{660}}$$
$$B_{28}=\frac{C_{180}C_{210}-C_{280}C_{110}}{H},\ H=C_{110}C_{220}-C_{120}C_{210},$$
$$b_{32}=-\frac{2C_{661}}{C_{660}},\ b_{35}=\frac{C_{350}}{C_{660}},\ b_{38}=\frac{C_{380}}{C_{660}}, \tag{A.3}$$
$$C_{11i_1}=\int_{-h/2}^{h/2}Y_{11}^{\bar{z}}z^{i_1}\mathrm{d}z,\ C_{12i_1}=\int_{-h/2}^{h/2}Y_{12}^{\bar{z}}z^{i_1}\mathrm{d}z,$$
$$C_{21i_1}=\int_{-h/2}^{h/2}Y_{21}^{\bar{z}}z^{i_1}\mathrm{d}z,C_{22i_1}=\int_{-h/2}^{h/2}Y_{22}^{\bar{z}}z^{i_1}\mathrm{d}z,$$
$$C_{66i_1}=\int_{-h/2}^{h/2}Y_{66}^{\bar{z}}z^{i_1}\mathrm{d}z,\ C_{15i_2}=\int_{-h/2}^{h/2}I_1^zY_{11}^{\bar{z}}z^{i_2}\mathrm{d}z,$$
$$C_{18i_2}=\int_{-h/2}^{h/2}I_2^zY_{12}^{\bar{z}}z^{i_2}\mathrm{d}z,\ C_{25i_2}=\int_{-h/2}^{h/2}I_1^zY_{21}^{\bar{z}}z^{i_2}\mathrm{d}z,$$
$$C_{28i_2}=\int_{-h/2}^{h/2}I_2^zY_{22}^{\bar{z}}z^{i_2}\mathrm{d}z,\ C_{35i_2}=\int_{-h/2}^{h/2}I_1^zY_{66}^{\bar{z}}z^{i_2}\mathrm{d}z,$$
$$C_{38i_2}=\int_{-h/2}^{h/2}I_2^zY_{11}^{\bar{z}}z^{i_2}\mathrm{d}z,\ i_1=0,\ 1,\ 2;\ \ i_2=0,\ 1.$$

Appendix B

$$k_{11}=\overline{m}^2\left\{\frac{\delta_1\left[(A_{11}-A_{31})\overline{n}^2+A_{12}\overline{m}^2\right]}{B_{11}\overline{m}^4+(\mathrm{B}_{12}+B_{21}+B_{31})\overline{m}^2\overline{n}^2+B_{22}\overline{n}^4}-A_{13}\overline{m}^2\right.$$
$$\left.-\left(A_{14}+A_{32}\right)\overline{n}^2\right\},$$
$$k_{11}^{NL}=-\frac{2\overline{mn}}{3l_1l_2}\frac{A_{12}}{B_{22}}\lambda,\ k_{11}^t=-\rho_1\overline{m}^2,\ k_{12}=\overline{m}\left(A_{15}\overline{m}^2+A_{35}\overline{n}^2+I_3\right),$$
$$k_{12}^t=\rho_2\overline{m},$$
$$k_{13}=(A_{18}+A_{38})\overline{m}^2\overline{n},$$
$$k_{21}=\overline{n}^2\left\{\frac{\delta_1\left[A_{21}\overline{n}^2+(A_{22}-A_{31})\overline{m}^2\right]}{B_{11}\overline{m}^4+(B_{12}+B_{21}+B_{31})\overline{m}^2\overline{n}^2+B_{22}\overline{n}^4}\right.$$
$$\left.-\left(A_{32}+A_{23}\right)\overline{m}^2-A_{24}\overline{n}^2\right\},$$
$$k_{21}^{NL}=-\frac{2\overline{mn}}{3l_1l_2}\frac{A_{21}\lambda}{B_{11}},\ \ k_{21}^t=-\rho_1\overline{n}^2,k_{22}=(A_{25}+A_{35})\overline{n}^2\overline{m},$$
$$k_{23}=\overline{n}\left(A_{28}\overline{n}^2+A_{38}\overline{m}^2+I_4\right),$$
$$k_{23}^t=\rho_3\overline{n},\ k_{31}=\frac{\delta_1\left(\overline{m}^2/R_2+\overline{n}^2/R_1\right)}{B_{11}\overline{m}^4+(B_{12}+B_{21}+B_{31})\overline{m}^2\overline{n}^2+B_{22}\overline{n}^4},$$
$$k_{32}=\frac{1}{16}\left(\frac{\overline{n}^4}{B_{22}}+\frac{\overline{m}^4}{B_{11}}\right),$$
$$k_{31}^{NL}=-\frac{1}{12l_1l_2}\left[\frac{1}{R_2}\frac{1}{B_{22}}\frac{\overline{n}}{\overline{m}}+\frac{1}{R_1}\frac{1}{B_{11}}\frac{\overline{m}}{\overline{n}}\right.$$
$$\left.+\frac{32\delta_1\overline{mn}}{B_{11}\overline{m}^4+(\mathrm{B}_{12}+B_{21}+B_{31})\overline{m}^2\overline{n}^2+\mathrm{B}_{22}\overline{n}^4}\right]\lambda,$$
$$k_{33}=I_3\overline{m},\ k_{34}=I_4\overline{n},\ \ \lambda=\left[(-1)^{m+n}-(-1)^m-(-1)^n+1\right] \tag{B.1}$$

References

[1] VA. Lomakin, Theory of Elasticity of Inhomogeneous Bodies, Publishing House of Moscow State University, Moscow, 1976.

[2] YM. Grigorenko, AT. Vasilenko, ND. Pankratova, Problems of the Elasticity Theory of Heterogeneous Bodies, Naukova Dumka, Kiev, 1991.

[3] J. Awrejcewicz, AV. Krysko, SA. Mitskevich, MV. Zhigalov, VA. Krysko, Nonlinear dynamics of heterogeneous shells. Part 2. Chaotic dynamics of variable thickness shells, Int. J. Non-Linear Mech. 129 (2021) 103660.

[4] HS. Shen, Functionally graded materials, in: Nonlinear Analysis of Plates and Shells, CRC Press, Florida, 2009.

[5] R. Kawamura, D. Huang, Y. Tanigawa, Thermoelastic deformation and stress analyses of an orthotropic nonhomogeneous rectangular plate, in: Proceedings of Fourth International Congress on Thermal Stresses 2001, pp. 189–192.

[6] GH. Paulino, JH. Kim, Isoparametric graded finite elements for nonhomogeneous isotropic and orthotropic materials, J. Appl. Mech. 69 (2002) 502–514.

[7] AH. Sofiyev, M. Omurtag, E. Schnack, The vibration and stability of orthotropic conical shells with non-homogeneous material properties under a hydrostatic pressure, J. Sound Vib. 319 (3–5) (2009) 963–983.

[8] AY. Grigorenko, NP. Yaremchenko, SN. Yaremchenko, Analysis of the anisotropic stress–strain state of a continuously inhomogeneous hollow sphere, Int. Appl. Mech. 54 (5) (2008) 577–583.

[9] J. Awrejcewicz, AV. Krysko, SA. Mitskevich, MV. Zhigalov, VA. Krysko, Nonlinear dynamics of heterogeneous shells Part 1. Statics and dynamics of heterogeneous variable stiffness shells, Int. J. Non-Linear Mech. 130 (2021) 103669.

[10] SA. Ambartsumian, Theory of Anisotropic Shells, State Publishing House for Physical and Mathematical Literature, Moscow, 1961.

[11] JN. Reddy, Mechanics of Laminated Composite Plates and Shells: Theory and Analysis, second ed., CRC Press, New York, 2004.

[12] F. Tornabene, M. Viscoti, R. Dimitri, JN. Reddy, Higher order theories for the vibration study of doubly-curved anisotropic shells with a variable thickness and isogeometric mapped geometry, Compos. Struct. 267 (2021) 113829.

[13] M. Amabili, Nonlinear vibrations and stability of laminated shells using a modified first-order shear deformation theory, Eur. J. Mech. A-Solids 68 (2018) 75–87.

[14] AH. Sofiyev, Application of the first order shear deformation theory to the solution of free vibration problem for laminated conical shells, Compos. Struct. 188 (2018) 340–346.

[15] AS. Volmir, The Nonlinear Dynamics of Plates and Shells, Nauka, Moscow, 1972.

[16] M. Amabili, Nonlinear Vibrations and Stability of Shells and Plates, Cambridge University Press, New York, 2008.

[17] C. Du, Y. Li, X. Jin, Nonlinear forced vibration of functionally graded cylindrical thin shells, Thin-Walled Struct. 78 (2014) 26–36.

[18] GG. Sheng, X. Wang, The non-linear vibrations of rotating functionally graded cylindrical shells, Nonlinear Dynam. 87 (2017) 1095–1109.

[19] GG. Sheng, X. Wang, Nonlinear vibrations of FG cylindrical shells subjected to parametric and external excitations, Compos. Struct. 191 (2018) 78–88.

[20] M. Avey, A.H. Sofiyev, N. Fantuzzi, N. Kuruoglu, Primary resonance of double-curved nanocomposite systems using improved nonlinear theory and multi-scales method: modeling and analytical solution, Int. J. Nonlin. Mech. 137 (2021) 103816.
[21] M. Amabili, P. Balasubramanian, Nonlinear forced vibrations of laminated composite conical shells by using a refined shear deformation theory, Compos. Struct. 249 (2020) 112522.
[22] AH. Sofiyev, M. Avey, N. Kuruoglu, An approach to the solution of nonlinear forced vibration problem of structural systems reinforced with advanced materials in the presence of viscous damping, Mech. Syst. Signal Process. 161 (2021) 107991.
[23] AH. Sofiyev, F. Turan, N. Kuruoglu, Influences of material gradient and nonlinearity on the forced vibration of orthotropic shell structures, Compos. Struct. (2021) 114157, http://dx.doi.org/10.1016/j.compstruct.2021.114157.
[24] C. Zhu, X. Fang, G. Nie, Nonlinear free and forced vibration of porous piezoelectric doubly-curved shells based on NUEF model, Thin-Walled Struct. 163 (2021) 107678.
[25] C. Ye, YQ. Wang, Nonlinear forced vibration of functionally graded graphene platelet-reinforced metal foam cylindrical shells: internal resonances, Nonlinear Dynam. (2021) http://dx.doi.org/10.1007/s11071-021-06401-7.
[26] Y. Liu, Z. Qin, F. Chu, Nonlinear forced vibrations of FGM sandwich cylindrical shells with porosities on an elastic substrate, Nonlinear Dynam. 104 (2) (2021) 1007–1021.
[27] R. Gao, X. Sun, H. Liao, Y. Li, DN. Fang, Symplectic wave-based method for free and steady state forced vibration analysis of thin orthotropic circular cylindrical shells with arbitrary boundary conditions, J. Sound Vib. 491 (2021) 115756.
[28] H. Ahmadi, A. Bayat, ND. Duc, Nonlinear forced vibrations analysis of imperfect stiffened FG doubly curved shallow shell in thermal environment using multiple scales method, Compos. Struct. 256 (2021) 113090.
[29] AH. Nayfeh, DT. Mook, Nonlinear Oscillations, John Wiley, New York, 1979.
[30] HT. Thai, SE. Kim, Levy-type solution for free vibration analysis of orthotropic plates based on two variable refined plate theory, Appl. Math. Model. 36 (2012) 3870–3882.
[31] M. Amabili, F. Pellicano, Nonlinear vibrations and multiple resonances of fluid-filled, circular shells, Part 1: equations of motion and numerical results, J. Vib. Acoust. 122 (4) (2000) 346–354.